

PL-TR-97-2053

**ADVANCED FTIR SIGNAL PROCESSING FOR  
AIRBORNE AND SPACEBORNE REMOTE SENSING  
OF CHEMICAL CLOUDS**

**Hans Malik**

**AIL Systems, Inc.  
Commack Road  
Deer Park, New York 11729**

**22 July 1997**

**19971021 235**

**FINAL REPORT  
July 1995 - March 1997**

**DTIC QUALITY INSPECTED 2**

**Approved for Public Release; distribution unlimited**



**PHILLIPS LABORATORY  
Directorate of Geophysics  
AIR FORCE MATERIEL COMMAND  
HANSCOM AFB, MA 01731-3010**

"This technical report has been reviewed and is approved for publication"

*Ray Huppi*

(Signature)  
Ray Huppi  
Contract Manager

*Donald K. Smith*

(Signature) *acting for*  
Stephen Price  
Branch Chief

*William Blumberg*

(Signature)  
William Blumberg  
Division Director

This report has been reviewed by the ESC Public Affairs Office (PA) and is releasable to the National Technical Information Service (NTIS).

Qualified requesters may obtain additional copies from the Defense Technical Information Center (DTIC). All others should apply to the National Technical Information Service (NTIS).

If your address has changed, if you wish to be removed from the mailing list, or if the addressee is no longer employed by your organization, please notify PL/IM, 29 Randolph Road, Hansom AFB, MA 01731-3010. This will assist us in maintaining a current mailing list.

Do not return copies of this report unless contractual obligations or notices on a specific document require that it be returned.

# REPORT DOCUMENTATION PAGE

Form Approved  
OMB No. 0704-0188

Public reporting burden for this collection of information is estimated to average 1 hour per response, including the time for reviewing instructions, searching existing data sources, gathering and maintaining the data needed, and completing and reviewing the collection of information. Send comments regarding this burden estimate or any other aspect of this collection of information, including suggestions for reducing this burden, to Washington Headquarters Services, Directorate for Information Operations and Reports, 1215 Jefferson Davis Highway, Suite 1204, Arlington, VA 22202-4302, and to the Office of Management and Budget, Paperwork Reduction Project (0704-0188), Washington, DC 20503.

1. AGENCY USE ONLY (Leave blank)	2. REPORT DATE	3. REPORT TYPE AND DATES COVERED
	22 July 1997	Final (July 1995–March 1997)
4. TITLE AND SUBTITLE		5. FUNDING NUMBERS
Advanced FTIR Signal Processing for Airborne and Space-borne Remote Sensing of Chemical Clouds		PE 63716D PR SERD TA BB WU AA
6. AUTHOR(S)		Contract F19628-95-C-0120
Hans Malik		
7. PERFORMING ORGANIZATION NAME(S) AND ADDRESS(ES)		8. PERFORMING ORGANIZATION REPORT NUMBER
AIL Systems, Inc Commack Road Deer Park, New York 11729		
9. SPONSORING/MONITORING AGENCY NAME(S) AND ADDRESS(ES)		10. SPONSORING/MONITORING AGENCY REPORT NUMBER
Phillips Laboratory 29 Randolph Road Hanscom AFB, MA 01731-3010		PL-TR-97-2053
Contract Manager: Ray Huppi/GPOS		
11. SUPPLEMENTARY NOTES		

12a. DISTRIBUTION/AVAILABILITY STATEMENT	12b. DISTRIBUTION CODE
Approved for public release; distribution unlimited	

## 13. ABSTRACT (Maximum 200 words)

The feasibility of using a Fourier Transform Infrared (FTIR) spectrometer from an airborne platform for remote sensing of air pollution was investigated. Air Force Phillips Laboratory mounted a FTIR spectrometer into a small twin engine aircraft and obtained the data used in this investigation. The aircraft was flown over sections of New York and New England. The spectrometer was operated in two different configurations, a passive configuration where the spectrometer viewed the warm ground and atmosphere below the aircraft, and an extractive mode where outside air was flushed through a 100 meter optical path gas cell. The spectral data were analyzed at AIL Systems Inc. for the presence of atmospheric pollutants. Various analysis techniques were investigated including Probabilistic Neural Networks (PNN), Principal Component

14. SUBJECT TERMS	15. NUMBER OF PAGES		
Infrared spectroscopy	36		
Air pollution			
FTIR			
16. PRICE CODE			
17. SECURITY CLASSIFICATION OF REPORT	18. SECURITY CLASSIFICATION OF THIS PAGE	19. SECURITY CLASSIFICATION OF ABSTRACT	20. LIMITATION OF ABSTRACT
Unclassified	Unclassified	Unclassified	SAR

Analysis (PCA) and Classical Least Squares (CLS). Background removal to remove the strong spectral features of water vapor and carbon dioxide followed by CLS was found to be the most suitable technique. Pollutants detected included ozone, carbon monoxide, oxides of nitrogen, methanol, and ammonia.

## CONTENTS

<b>1. Introduction</b>	<b>1</b>
<b>2. Passive FTIR for Chemical Detection</b>	<b>1</b>
2.1 Available Radiance	2
2.2 Radiance at Input	2
2.3 Atmospheric Effects	3
2.4 Instrumental response	3
2.4.1 NESR as Critical Instrument Parameter	4
2.5 Environmental Chemicals of Interest	4
2.6 Detection Methods and Algorithms	4
2.6.1 Amplitude Threshold	5
2.6.2 CLS	5
2.6.3 PNN	5
2.6.4 PCA	6
2.6.5 The $I_0$ Problem	6
<b>3. Ground Based FTIR Measurements</b>	<b>7</b>
3.1 Instrument NESR	7
3.1.1 Differential Near Room Temperature	8
3.1.2 Differential Relative to LN2	8
3.2 Radiances	9
3.3 Chemicals	11
<b>4. Fall Airborne Passive Measurements</b>	<b>11</b>
4.1 Estimation of NESR During Flight	11
4.2 NESR (Ground & Flight)	12
4.3 Apparent Radiance Contrasts	12
4.4 Chemicals	12
<b>5. Summer Airborne Extractive Measurements</b>	<b>13</b>
5.1 Active FTIR vs. Passive	14
5.2 NEA (Ground & Flight)	14
5.3 Chemicals	14
5.3.1 <u>Ozone</u>	14
5.3.2 <u>Ammonia</u>	16
5.3.3 <u>Carbon Monoxide</u>	18
5.3.4 <u><math>N_2O</math></u>	19
5.3.5 <u><math>NO_2</math></u>	19
5.3.6 <u><math>SO_2</math></u>	21
5.4 Implications for Passive Detection	22
5.4.1 <u>Ozone</u>	23
5.4.2 <u>Ammonia</u>	23
5.4.3 <u><math>SO_2</math></u>	24
5.4.4 <u><math>NO_x</math></u>	24
<b>6. Summer Airborne Passive Measurements</b>	<b>24</b>
6.1 NESR During Flight	24
6.2 Apparent Radiance Contrasts	25
6.3 Chemicals	25
<b>7. Conclusions for Passive FTIR for Environmental Monitoring</b>	<b>29</b>
7.1 <u>Ozone</u>	29
7.2 <u>Ammonia</u>	29
7.3 <u><math>SO_2</math></u>	30
7.4 <u><math>N_2O</math></u>	31
7.5 <u>Methanol</u>	31
7.6 <u>Aliphatic Hydrocarbons</u>	31
7.7 <u>Aromatic Hydrocarbons</u>	31
7.8 <u>Other</u>	32
7.9 <u>Conclusion</u>	32

## 1. Introduction

This is the final report for contract F19628-95-C-0120. The purpose of the contract was to evaluate the feasibility of using passive FTIR for the monitoring of environmentally significant vapors and gases. The study used an FTIR with  $0.5\text{ cm}^{-1}$  resolution manufactured by the MIDAC corporation. The instrument was operated as an airborne passive FTIR, both in the winter and the summer. Ground based measurements were made prior to the airborne measurements to baseline the instrument. Also, measurements were made using the instrument in an extractive mode, measuring the actual chemical concentrations in the air outside the aircraft. This is used to help interpret the airborne measurements done later.

The aircraft was flown over sections of New York and New England, with the interferometer usually looking downward. The instrument was viewing out a port in the side of the plane. The instrument averages the measurement over the field of view (FOV) projected onto the ground, and averages the measurement over the path the aircraft covered in one scan time. The FOV of the interferometer is roughly  $1^\circ$  (17 mrad). Thus, at 1000 meters the footprint is 17 meters.

Airspeed was about 140 knots (260 kph). The roughly 1.57 seconds between scans implies that each data acquisition takes place over  $\sim 100$  meters, with  $\sim 10$ -20 meters of dead time between scans. A concentration grid developed from single scans is therefore  $\sim 0.1$  Km cells, whereas a grid developed of 64 coadded scans is  $\sim 7\frac{1}{4}$  Km grid.

In passive FTIR measurements, ozone and possibly methanol, were detected, with the ozone the more consistent. Also, some spectra of unknown origin were observed near Monsanto. The concentrations of the chemicals measured with the extractive system are consistent with the data from the passive, both for the detected chemicals and the chemicals that were unobserved with the passive FTIR. The data is also consistent with the EPA reported air quality for the days in question, and the PAM station information for the days in question.

Ozone and other environmental chemicals can be mapped with airborne passive FTIR, with a spatial resolution depending on the airspeed of the platform. If the chemicals are broadly distributed, coadding of the spectra can be used to improve the detection limits of the instrument. Because the signal level is dependent on the total amount of the chemical between the aircraft and the ground, and the temperature contrast between the air and the ground, the calculation of the concentration at ground level is problematic. Measurement of the signals at various altitudes, and a good knowledge of the instrument response would enable quantification of the average concentration in strata (e.g. 0-1000'; 1000-2000'; etc.)

In addition the extractive measurements provide a useful data base for evaluation of current models of the distribution of pollutants in the atmosphere, along with their usefulness in mapping chemical concentrations at various altitudes and locations for both research and regulatory purposes.

## 2. Passive FTIR for Chemical Detection

Passive infrared detection of chemicals relies on the thermal radiation from the atmosphere, or from the earth, to provide a signal level. The signal of interest is related to

the amount of chemical (in molecules/area) and the “available radiance”. The available radiance is related to the difference in temperature between the atmosphere and the background. When the platform is looking at the ground this temperature contrast is usually only a few degrees out of 300.

## 2.1 Available Radiance

The available radiance, for a background of emissivity 1, is calculable from the following formula.:

$$I_{\text{result}} = I(T_{\text{Background}}) * \tau + (1-\tau) * I(T_{\text{Atmosphere}}) \quad (1)$$

Where the  $I(T)$ s are the blackbody radiances from objects at those temperatures,  $\tau$  is the transmittance of the atmosphere. This can be simplified in the case where the emissivity of the background is one, and the background is warmer than the air. For that case the equation for the incoming radiance is:

$$I = I(T_{\text{Atmosphere}}) + \tau * (I(T_{\text{Background}}) - I(T_{\text{Atmosphere}})) \quad (2)$$

Notice that the maximum amount of signal due to chemical absorption is the difference in radiance between the two blackbodies, which can be seen in Figure 1.

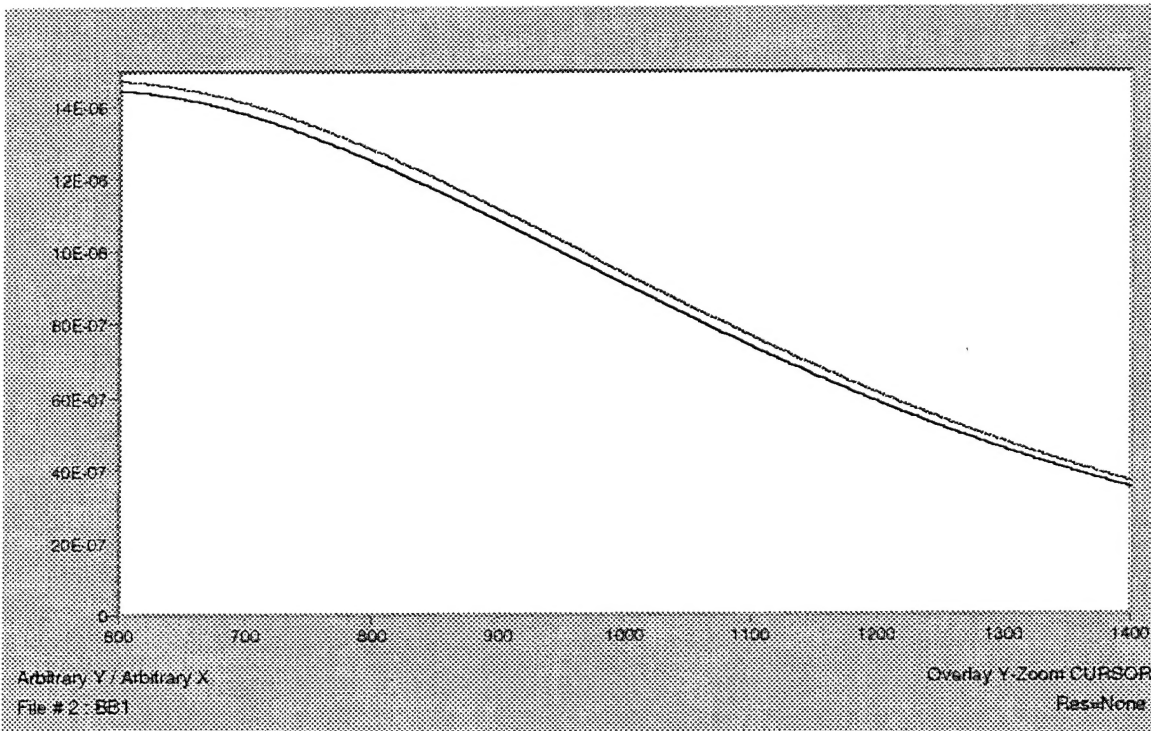


**Figure 1 Available Radiance From 297°, 295° Blackbodies**

## 2.2 Radiance at Input

The radiance expected at the instrument can be calculated from the above equation. Using the same assumptions as above, the radiance with a chemical in the atmosphere is:

$$I = I(T_{\text{Atmosphere}}) + e^{-\alpha CL} (I(T_{\text{Background}}) - I(T_{\text{Atmosphere}})) \quad (3)$$

where  $\alpha CL$  is the absorbance of the amount of chemical present.

### 2.3 Atmospheric Effects

The atmosphere has two main methods of loss in signal. There is an overall loss in signal level due to aerosol scatter and the molecular continuum, and there is absorption at specific chemical lines that will interfere with the detection of specific chemicals.

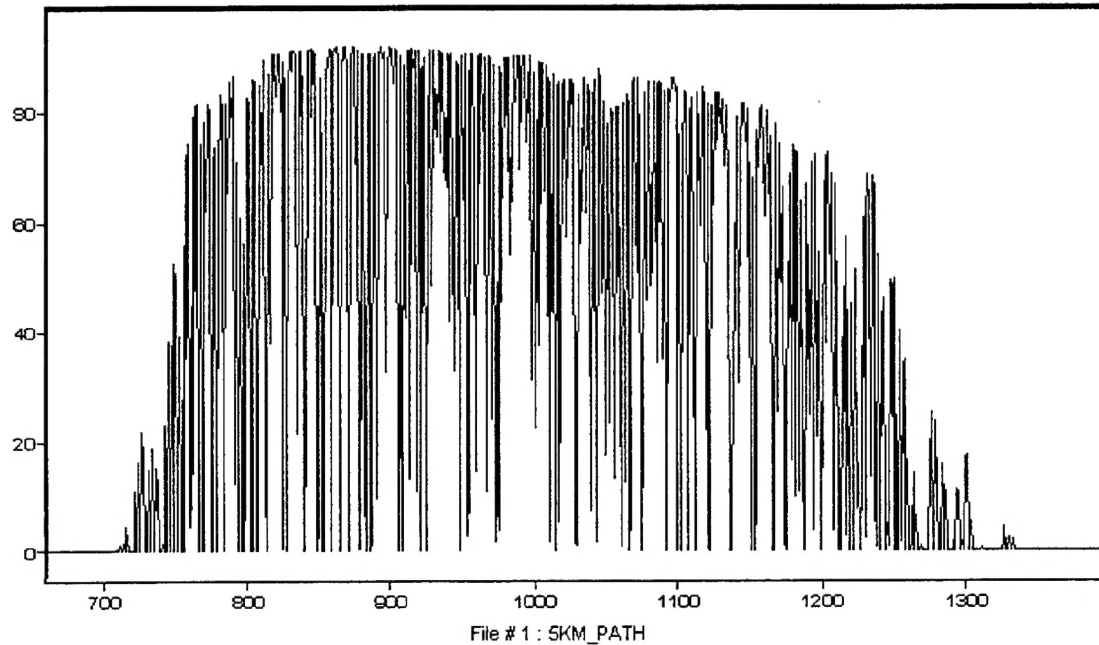


**Figure 2 Atmospheric Transmission**

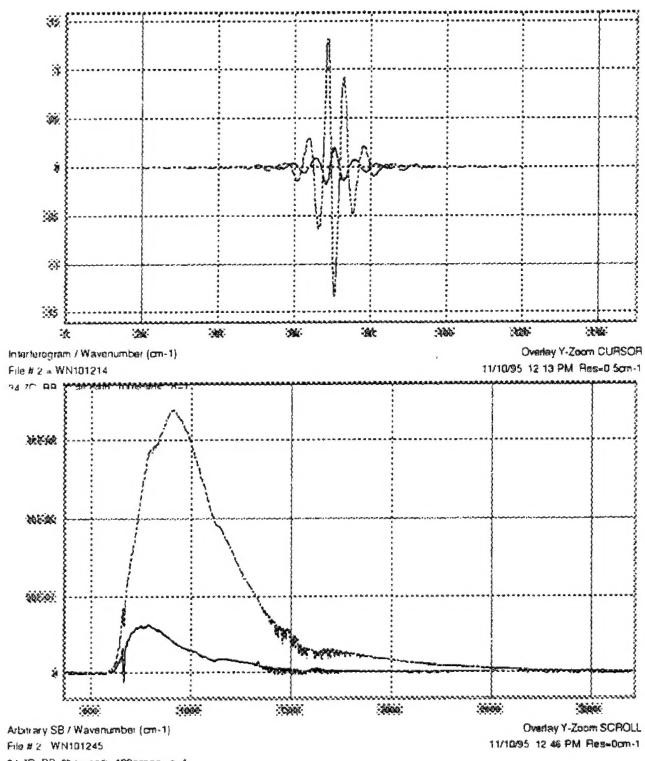
The atmosphere has very little transmission in the infrared, except between 750 and 1250 cm⁻¹, as can be seen in Figure 2

### 2.4 Instrumental response

The signal from the interferometer is a function of the external radiance and the instrument response function (IRF). The IRF is calculated from the difference of two or more measurement of the instrument with different calibrated Blackbody sources. The following formula was used to calculate the IRF.

$$IRF = \frac{Signal(T_1) - Signal(T_2)}{Radiance(T_1) - Radiance(T_2)} \quad (4)$$

Because the signal from the instrument is a function of both internal and external radiances, the differential is necessary to accurately measure the response to a change in external signal. The magnitude of the effect is shown in Figure 3.



Cold Interferogram (77K), and 34.7°C Interferogram.

Cold Spectrum (77K), and 34.7°C Spectrum.

**Figure 3 Internal Radiance Can Significantly Affect Measurements**

#### 2.4.1 NESR as Critical Instrument Parameter

The sensitivity of the instrument to a change in external radiance can be quantified by a parameter known as the Noise Equivalent Spectral Radiance (NESR). This is the change in input signal level (in  $\text{W}/\text{cm}^2 \text{sr cm}^{-1}$ ) that is equal to the RMS noise in the instrument. For a passive FTIR this is the critical measure of instrument sensitivity.

#### 2.5 Environmental Chemicals of Interest

The chemicals of interest are the EPA monitored chemicals such as ozone,  $\text{N}_2\text{O}$ , and  $\text{SO}_2$ . Other chemicals of environmental interest are aromatic VOCs such as Benzene and Toluene, aliphatic VOCs such as isobutane, and other chemicals such as methanol and ammonia.

#### 2.6 Detection Methods and Algorithms

A number of detection algorithms were investigated during this program. The more advanced methods of signal processing such as probabilistic Neural Networks (PNN), or Principal Component Analysis (PCA), require a training set of spectra with varying amounts of the chemical of interest. This training set should ideally be generated with the instrument in various realistic field conditions, although it can be generated from laboratory measurements. Without a previously generated training set of data, PNN and PCA cannot be used.

Most chemical detection algorithms are not applied to either the interferogram, or the raw spectrum. Most are applied either to the ratio or the difference of two spectra in order to remove the large blackbody component and be left with (hopefully) only chemical absorptions. The accurate removal of the background ( $I_0$ ), especially as the background temperature is changing from scan to scan, is a common issue in most detection algorithms. The method of background removal will affect the detection limits of any algorithm.

Five methods of background removal were investigated.

- 1) Ratio to a previously collected spectrum
- 2) Ratio to a known blackbody measurement, scaled by the apparent temperature differences.
- 3) Subtract two adjacent spectra.
- 4) Estimation of the Scene Blackbody temperature, and removal of that curve, correctly accounting for the IRF and the internal radiance, using measurements of a number of blackbodies at known temperatures.
- 5) Additional removal of the baseline error with a lower order polynomial fit.

### **2.6.1 Amplitude Threshold**

The easiest method of data analysis for detection of chemical spectra in passive FTIR is a thresholding of the “absorbance” spectrum. The “absorbance” spectrum can be generated by any of the  $I_0$  removal techniques described above. Features significantly above the noise level are compared, in location, to a list of line centers of chemicals of interest. In general, this method does not work well due to the large residual that usually occurs after the background removal.

### **2.6.2 CLS**

Classical Least Squares (CLS) uses a least squares fit to the shape of the absorbance curve for the chemicals of interest, to determine the concentration. This apparent concentration is compared to the error in the fit to that concentration to determine whether the detection is valid. CLS is significantly more useful than thresholding for a number of reasons: it has a threshold that depends on the noise in that specific scan, in the region of interest; it can remove first and second order errors in the residual baseline; it fits to the shape of the curve, not just a point, therefore lowering the false alarm rate.

### **2.6.3 PNN**

A Probabilistic Neural Network (PNN) carries out a pattern recognition process, separating the spectra into sets. This is done by using the values in the bins in an appropriate region as input vectors for the PNN. After suitable training, the PNN computes probabilities that the current spectrum matches to a previously categorized spectrum. A probability threshold is established to automatically distinguish scans with signal scans from background scans.

Probabilistic Neural Networks (PNN) can be better at pattern recognition than CLS, but they require a significant amount of data to train the algorithm for a chemical. There will also be several iterations in order to optimize the degree of training required. Too little and the categories are vague, too much and the algorithm will reject spectra that do not

resemble the training data. In addition, PNNs work better if the training set has realistic errors in it, which is difficult to do for passive FTIR data.

Although PNNs divide data into sets, and provide a probability of matching, they do not quantify the amount of chemical present. For environmental monitoring purposes quantification is critical, without knowing if the detected amount of chemical is below or above safe levels the information is not useful for environmental safety purposes. Therefore, PNNs were not attempted on this program.

#### 2.6.4 PCA

Principal Component Analysis (PCA), and Partial Least Squares (PLS), are methods of categorizing spectra based upon decomposition of measured spectra into orthogonal axes. These axes are correlated to axes that were generated with the training data. The magnitude of correlation indicates the chemical concentration. Again, this method requires a large training set, and PCA works better if the training set includes known mixtures of the chemicals of interest. Unlike PNNs, PCA can quantify the amounts, and with an appropriate set of training data, can even do so if there are non-linear intensity responses. PCA was investigated, but not implemented, due to the lack of acceptable training data.

#### 2.6.5 The $I_0$ Problem

All of the above algorithms work with “absorbance” spectra. The background has already been removed by dividing by some signal without the chemical, or  $I_0$ . The practical difficulty in passive detection is often what  $I_0$  to use, and how to remove it, because there is always some residual that will affect the detection limits. On this job, it was found that the CLS results could be improved by removing a spectrum with the apparent temperature of the spectrum from the measured spectrum. A comparison was made on files with ozone, but with a series of different levels of coaddition, and therefore different SNRs. As shown in Table 1 below, an improvement was made in detection limits by a factor of 30% by removing a baseline with an  $I_0$  of more appropriate shape, and using CLS.

**Table 1 Comparison of Detection Limits using Differing Methods of Background Removal**

File	Coadds	(C/3 $\sigma$ ) Method 1	(C/3 $\sigma$ ) Method 2	(C/3 $\sigma$ ) Method 3
s201812	1	1.0	1.2	1.3
s201814	4	0.8	1.1	1.1
s201818	16	1.1	1.5	1.5
s201822	64	1.2	1.5	1.5
Average		1.0	1.3	1.35

Method 1 was removal of the background with an  $I_0$  that was a recent calibrated BB of similar temperature. Method 2 was removal of the background with an  $I_0$  that was a function of a recent calibrated BB measurement, scaled by the ratio of apparent temperature differences. The scaling was wavelength dependent to account for the different shape of the BB curve at different temperatures. The third method used a fourth order polynomial to remove the baseline curvature that was left after method 2. As can be seen the largest

difference was in using an  $I_0$  with a more appropriate apparent temperature. This method of background removal will improve nearly all detection algorithms.

### 3. Ground Based FTIR Measurements

Before flight measurements were taken, ground based measurements were taken to establish the instrument performance under more controlled conditions.

Measure of instrument parameters was made on the ground, accounting for the effects of the internal radiance of the instrument. The Instrument Response Function (IRF) was calculated, along with the NESR. These results can be used to baseline the airborne data.

#### 3.1 Instrument NESR

Measurement of instrument response should account for the internal radiance of the instrument. The instrument has a signal component due to its own internal radiance, as can be seen in Figure 4. This internal radiance is not in phase with the external radiance, and must be correctly removed when measuring the NESR.

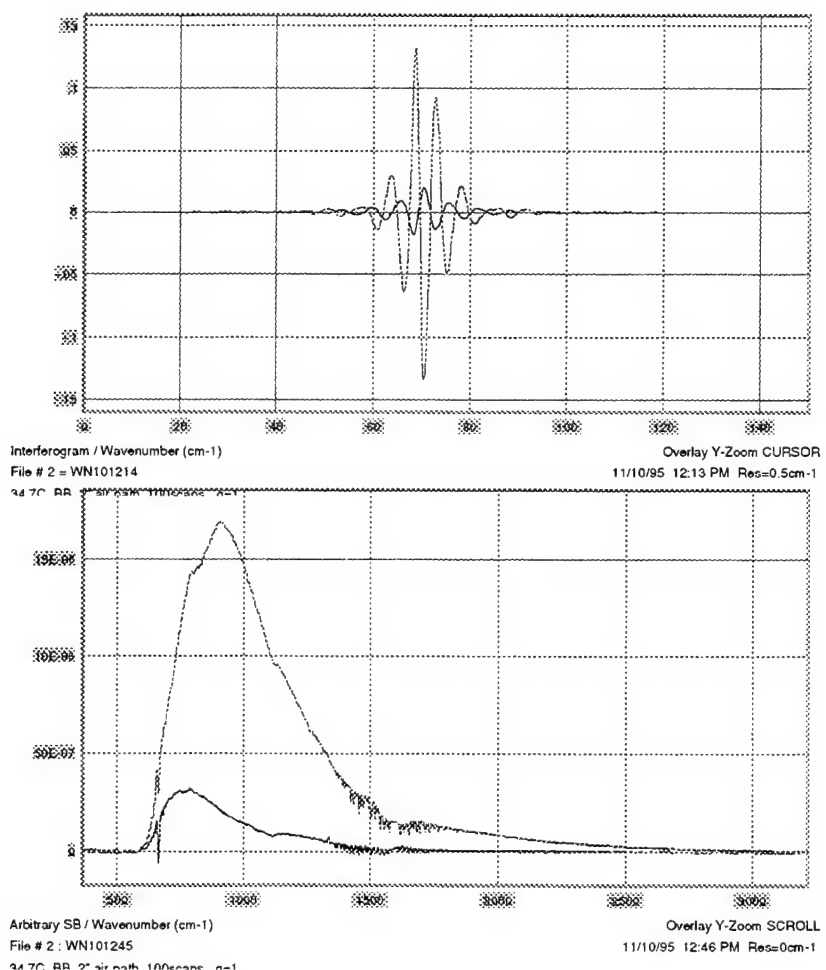


Figure 4 Responses Due To Internal And External Radiances

The height of the zero burst due to the internal radiance is about 1/7th the height of the zero burst due to a warm external source in the measurements shown. The peak height in spectral space is about 1/5 of the warm BB. At  $1000\text{ cm}^{-1}$  the instrument response is  $1.49\text{e-}5$  from the  $34.7\text{ }^{\circ}\text{C}$  BB, and  $1.43\text{e-}5$  from the cold BB. The response from the cold BB should be essentially zero.

### 3.1.1 Differential Near Room Temperature

NESR can be calculated from the IRF and the noise level of the instrument. The IRF calculated that way can be seen in Figure 5. The result is relatively noisy due to the differencing of spectra with nearly identical temperatures.

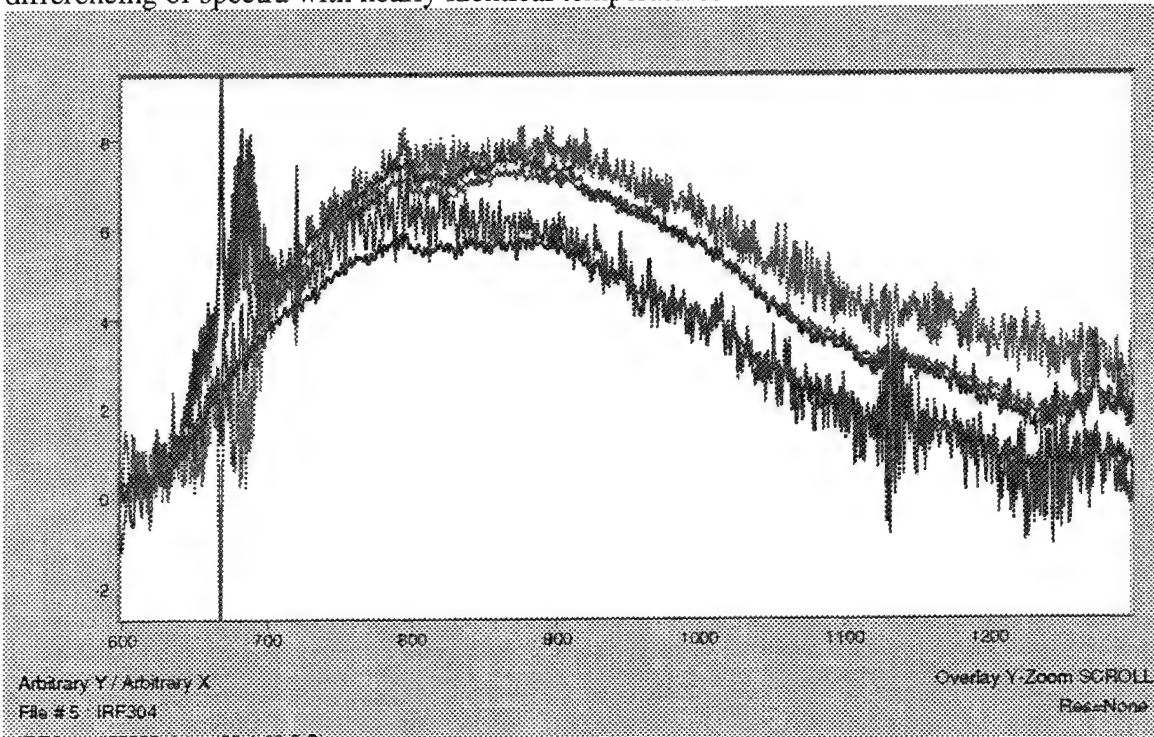
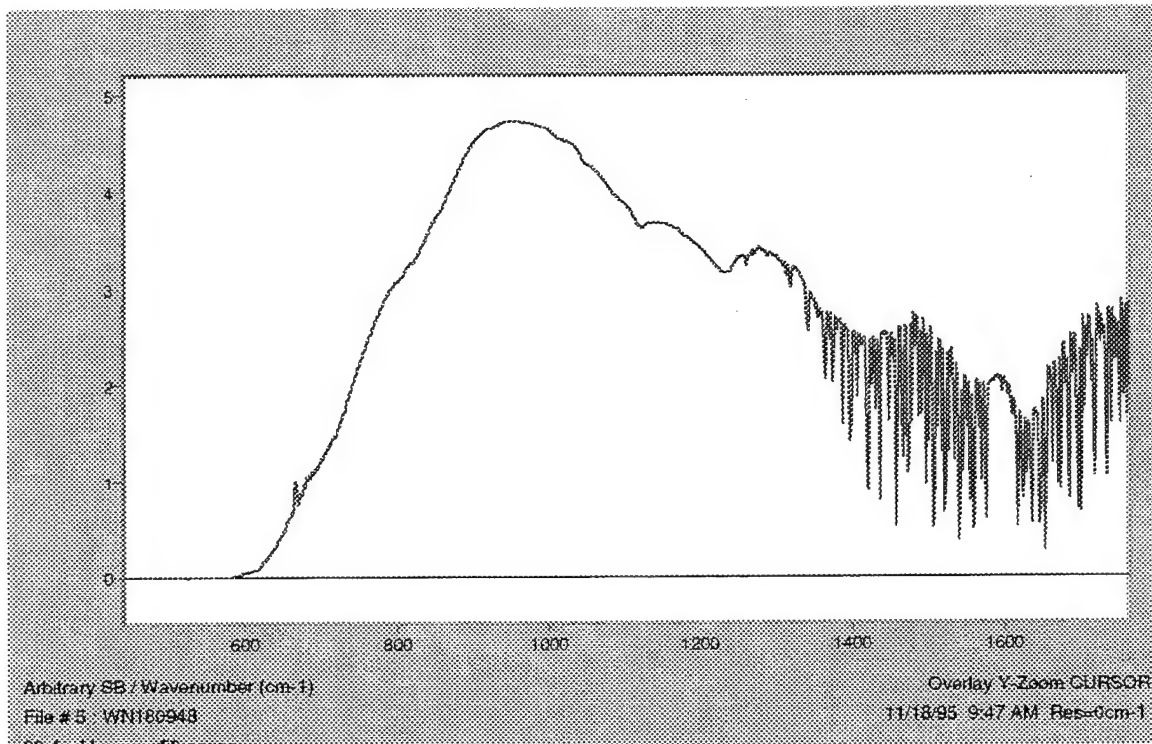


Figure 5 IRF From Differential Measurement Of Blackbodies Near R.T.

### 3.1.2 Differential Relative to LN2

Another way to measure the IRF is relative to an  $\text{LN}_2$  measurement, remembering to subtract the files in interferogram space, not spectral space. 1.2 is IRF (signal/(SR unit), this would be 5.0 for a 1 cm data point spacing. The better signal-to-noise in this measurement can be seen in Figure 4.



**Figure 6 IRF From LN<sub>2</sub> Measurement**

### 3.2 Radiances

In the ground measurements the effect of the temperature contrast were readily apparent. As can be seen in Figure 7, a measurement of the apparent radiance into the instrument looking across Rt. 128, there was little available radiance in some of the files. Figure 7 is the response in that file divided by the IRF. Figure 8 is the same result for a file collected across  $\sim 1000'$  path to woods. Note that the sky is apparent in the spectrum, as the lines are in significant emission, and ozone is quite apparent. In Figure 9, another scan across Rt.128, there is noticeable absorption. The  $1066\text{ cm}^{-1}$  water line, which should have significant absorption, has a depth of only about  $6 \times 10^{-7}\text{ W/cm}^2\text{sr}\text{cm}^{-1}$ , or less than 10 % of the signal level.

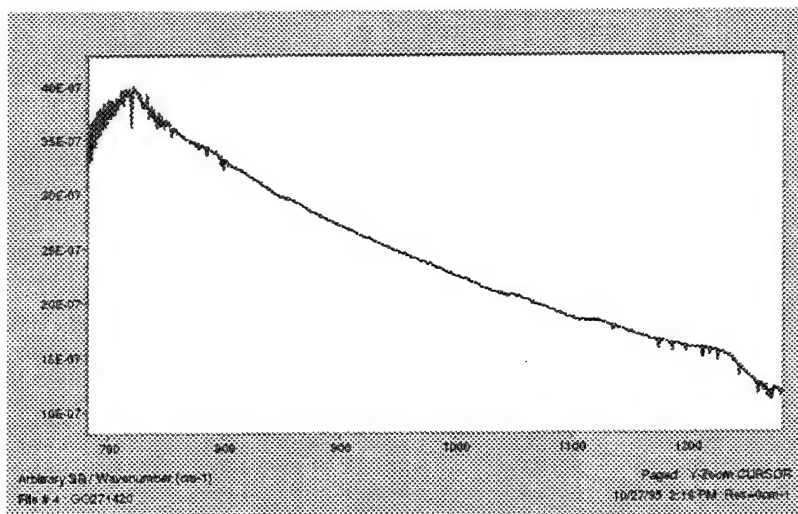


**Figure 7 Rt. 128 Traffic**

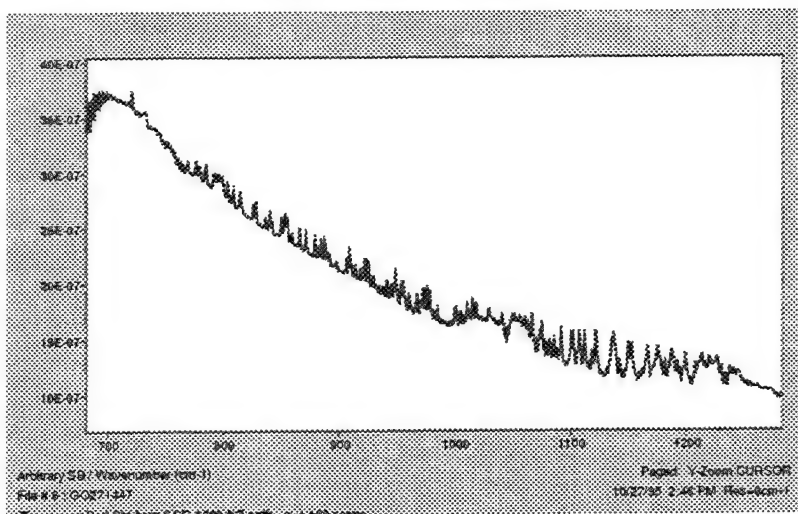


**Figure 8 Trees, ~1000' Path**

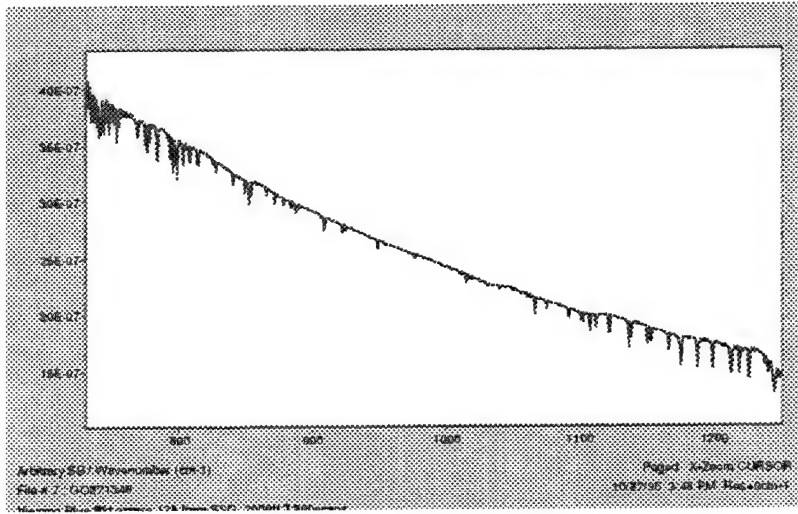


**Figure 9 2000' Scan Across Rt.128**

### 3.3 Chemicals

In the ground based measurements, a 1000' scan (O271452) had a significant amount of ozone, as shown in Figure 10.

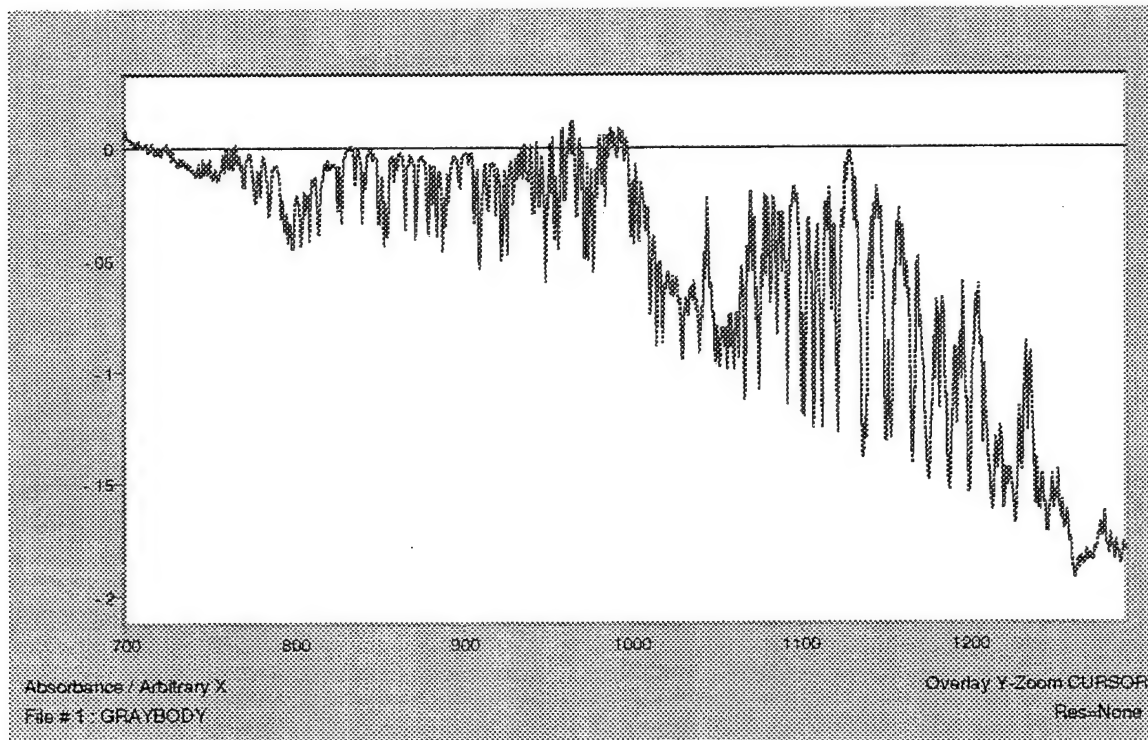


**Figure 10 1000' Path To Trees Shows Significant Ozone In Emission.**

## 4. Fall Airborne Passive Measurements

The first measurements were done in the fall. Measurements were taken both as single scans and co-added scans.

The fall measurements did not have many chemical detections, mostly because the concentrations of the chemicals of interest, such as ozone, and VOCs, were expected to be lower. Data from the PAM stations indicated that the majority of hydrocarbon concentrations were less than a few ppb. The highest concentration was about 3 ppb for ethane, but 1 ppb or less for the other chemicals. Ozone was not monitored by the PAM station during the fall.

### 4.1 Estimation of NESR During Flight

Because of the difficulty of performing NESR measurements in flight, instrument performance can be evaluated using the noise in the spectrum, and assuming that the IRF has remained constant since it was last measured. This can be done either by measuring the RMS noise out of band, or by subtracting two adjacent spectra, and measuring the RMS value of that ratio in a region of the spectrum without water lines (e.g. 968-1008  $\text{cm}^{-1}$ ).

#### **4.2 NESR (Ground & Flight)**

Before each flight a set of calibration data were taken. These were used to generate the IRF that was used to analyze that portion of the data. The NESR before take off was  $7 \times 10^{-9}$ , The NESR during flight varied, but was about  $2 \times 10^{-8}$  in scans from December 5th.

#### **4.3 Apparent Radiance Contrasts**

In the single scans from the flight data the average absorbed radiance from the  $1066 \text{ cm}^{-1}$  water line was only about  $3 \times 10^{-8} \text{ W/cm}^2 \text{ sr cm}^{-1}$ . Because this water line is expected to have very strong absorption, this implies a low temperature contrast for those measurements.

#### **4.4 Chemicals**

A number of chemicals were noted in the fall flight tests. Ozone and Methanol were noticed, along with possible detections of ethylene and an unknown hydrocarbon near Monsanto.

As shown in Figure 11 there was an unknown chemical noted several times. It was difficult to correlate this with a specific chemical, but it was similar to a 5-7 C long straight chain aliphatic hydrocarbon.

Methanol was possibly detected in a scan over a small town/residential area. Because methanol is a by-product of burning vegetation, this could be possible even if no chemical facilities were located nearby.

Ethylene might have been detected in a file collected about 20 minutes later on the way to the Beverly Airport.

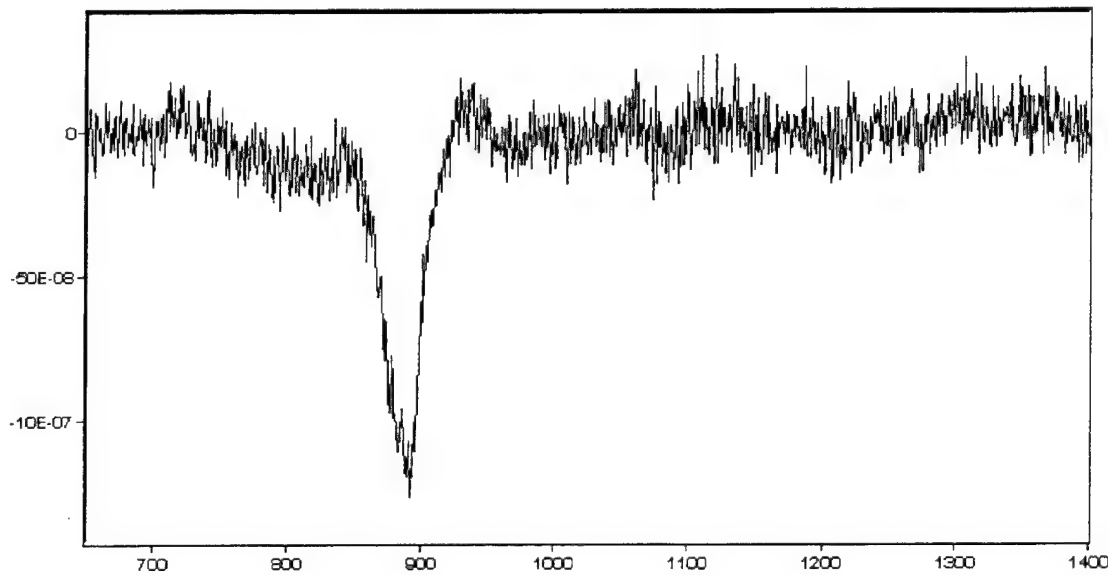


**Figure 11 Unknown Spectrum Collected Near Monsanto**

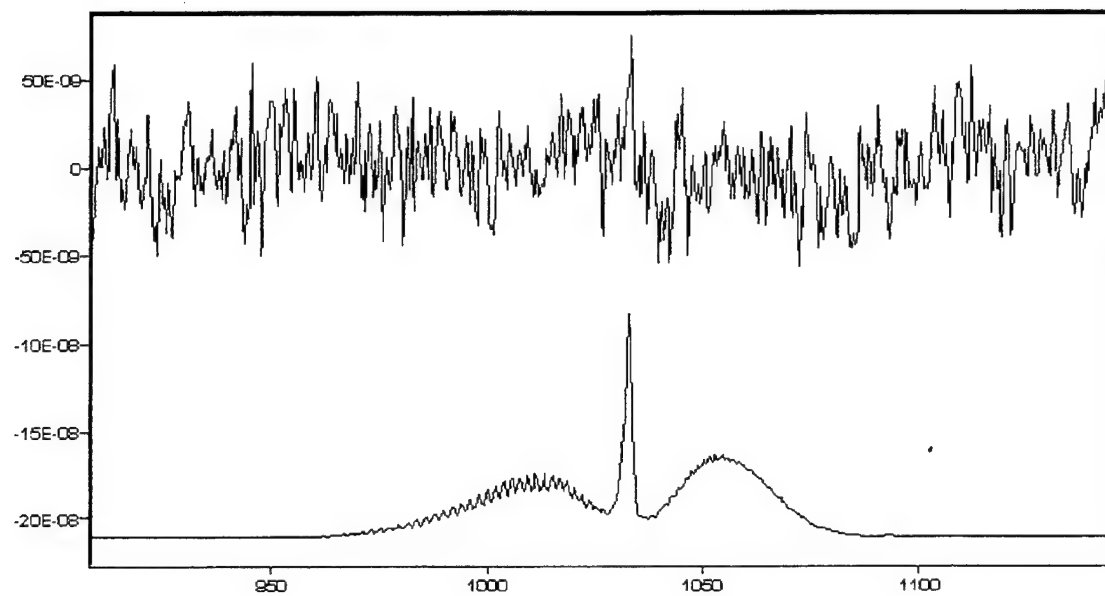


**Figure 12** File N181350 scan 59 May Contain Methanol

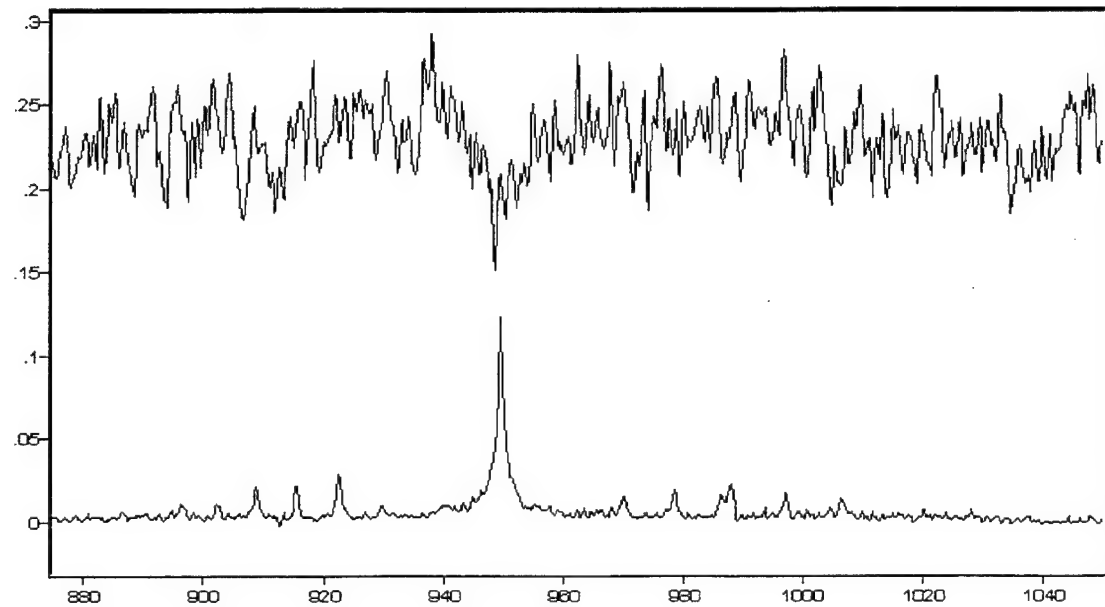


**Figure 13** File N181415 May Contain Ethylene

## 5. Summer Airborne Extractive Measurements

In the summer the aircraft was flown over similar regions, but the interferometer was used in an extractive mode, with a hot source. A number of chemicals were measured with this technique. Knowing the concentrations from these measurements, the detectabilities in passive measurements can be assessed.

## 5.1 Active FTIR vs. Passive

The extractive technique consisted of continuously flowing external air through a 100 meter White cell that was inside the aircraft. A high intensity IR source was shone through the cell, and an FTIR was used to determine the transmission of the extracted gasses. The active configuration that was used to do the extractive measurements had three advantages: it could provide a quantitative measure of the amount of chemical present; it could give a concentration at that location, not just the average over the path; signal was present out to  $4000\text{ cm}^{-1}$ , greatly increasing the number of chemicals that can be observed. The disadvantage is that it only measures concentration at the aircraft, not near ground level. In active measurements, the signal is also linearly related to the chemical concentration. In passive measurements, however, the temperature contrast is just as strong an effect as the concentration, and the internal radiance affects the total signal level by a significant amount. Both the temperature contrast and the internal radiance are both in general unknown in the measurement.

## 5.2 NEA (Ground & Flight)

The noise equivalent absorbance (NEA) of the extractive system during flight was 0.12 milliabsorbance units (for 128 coadded scans). This implies that the NEA for a single scan is 1.0 mAUs or less. Because the majority of the data was collected with 128 scan coaddition, the detection limits in the collected spectra is 0.12 mAUs. This is equivalent to a signal-to-noise ratio of about 3600:1 in transmission. This implies detection limits for the chemicals of interest.

## 5.3 Chemicals

### 5.3.1 Ozone

Ozone is observable in the  $1000\text{ cm}^{-1}$  to  $1060\text{ cm}^{-1}$  region, and is best characterized by the notable change in absorption at  $1042\text{ cm}^{-1}$ , as can be seen in Figure 14.

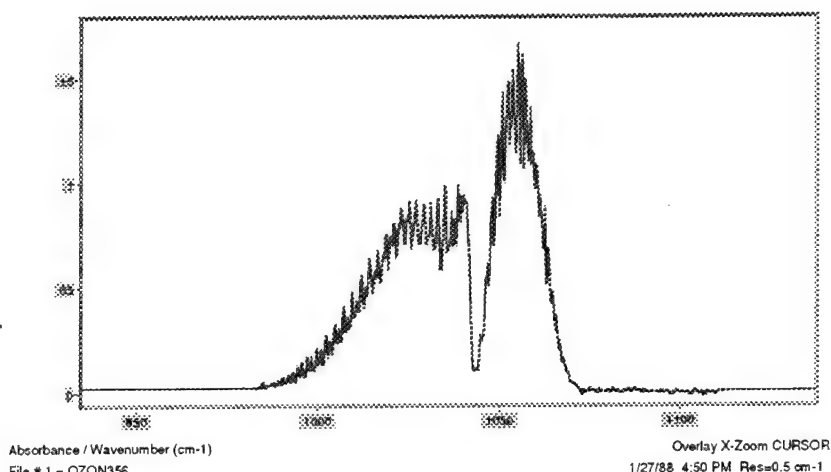


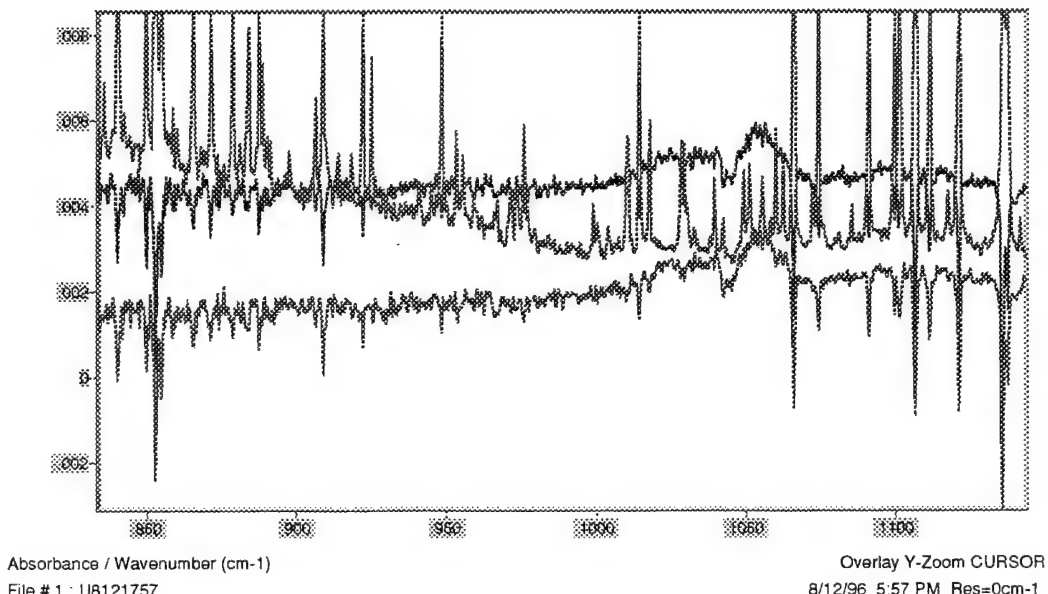
Figure 14 Ozone Reference Spectrum

In the scans near the Fall River Trash Burner and Brayton Power Plant (Figure 15, and Figure 16) the ozone concentration relative to a scan over Quabbin Reservoir is about 25 to 35 ppb. If the “normal” ozone concentration of 27 ppb (from HITRAN) is assumed for the background, this implies a 50 to 60 ppb concentration of Ozone in that region. At 700 meters altitude (a typical altitude for a later passive measurement) this is about 35 ppm\*m of ozone (50ppb\*700 meters). The files are listed in Table 2.

**Table 2 Ozone Concentrations Downwind of Power Plant**

<u>File:</u>	<u>Altitude:</u>	<u>Concentration (CLS):</u>	<u><math>3\sigma</math> (ppb)</u>
u8121801	1200'	34 ppb	3.5
u8121807	1200'	32 ppb	4.0
u8121813	2000'	0 ppb	2.0
u8121817	2000'	0 ppb	2.0
u8121823	3000'	0 ppb	2.4

Ozone noticed downwind of power plant.



files s8121807, s8121847, s8121813 over u8121849

**Figure 15 Some Of Scans Downwind Of Power Plant.**

## Quantitative Analysis of Ozone at 1200 ft (3.35 ppm\*m, 34.2 ppb)

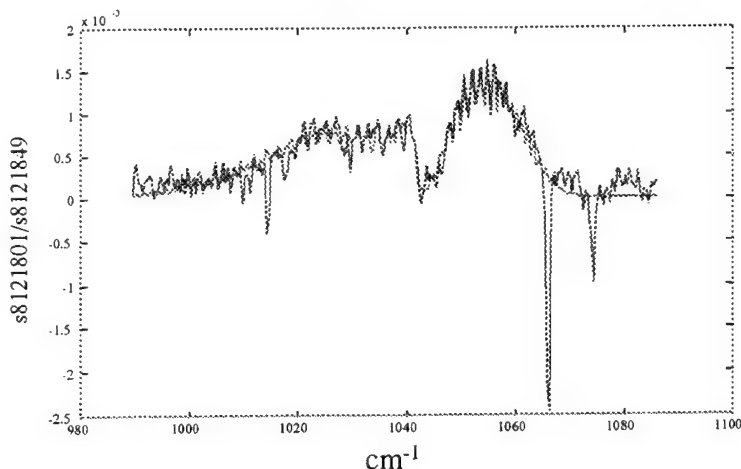


**Figure 16 CLS Fit Of Ozone Spectrum**

In addition, the files immediately preceding u8121801 also had significant amounts of ozone.

### 5.3.2 Ammonia

Ammonia is characterized by strong asymmetric lines at  $967\text{ cm}^{-1}$  and  $931\text{ cm}^{-1}$  and narrow lines at 992.7, 1046.5, and other locations (Figure 17). In the scans near Monsanto (Figure 18) the relative  $\text{NH}_3$  concentration is about 15 ppb at 1300' and about 10 ppb at 3000' when measured by absorbance height, as shown in Figure 19. The unlabeled spectrum (second from bottom) in that figure is an ammonia reference spectrum. Since HITRAN says atmospheric concentration is less than 1 ppb, the relative concentration is probably equal to the absolute concentration, although it should be noted that this is not true if the ammonia concentration over the Quabbin reservoir was significant. It should be noted as a general caveat that if the reference spectrum has the chemical of interest, then all of the generated absorbance spectra will appear to have that chemical, even if they have none of it, and all of the concentrations will be off by the amount in the reference spectrum. The HITRAN value, in conjunction with the measurement implies about 10 ppm\*m of ammonia for the passive measurements. The specific files are listed in

**Table 3 Files containing noticeable amounts of ammonia.**

<u>File:</u>	<u>Location:</u>	<u>Concentration (CLS):</u>	<u><math>3\sigma(\text{ppb})</math></u>
u8121634	Near Monsanto, 3000'	10 ppb	6.7
u8121640	Near Monsanto, 1300'	9 ppb	2.2
u8211646	Near Monsanto, 1300'	9 ppb	1.9
u8121651	Monsanto, in thermals, 1300'	8 ppb	1.7
u8121654	Monsanto, in thermals, 1300'	8 ppb	1.4

u8121659

Monsanto, in thermals, 1300'

7 ppb

1.3

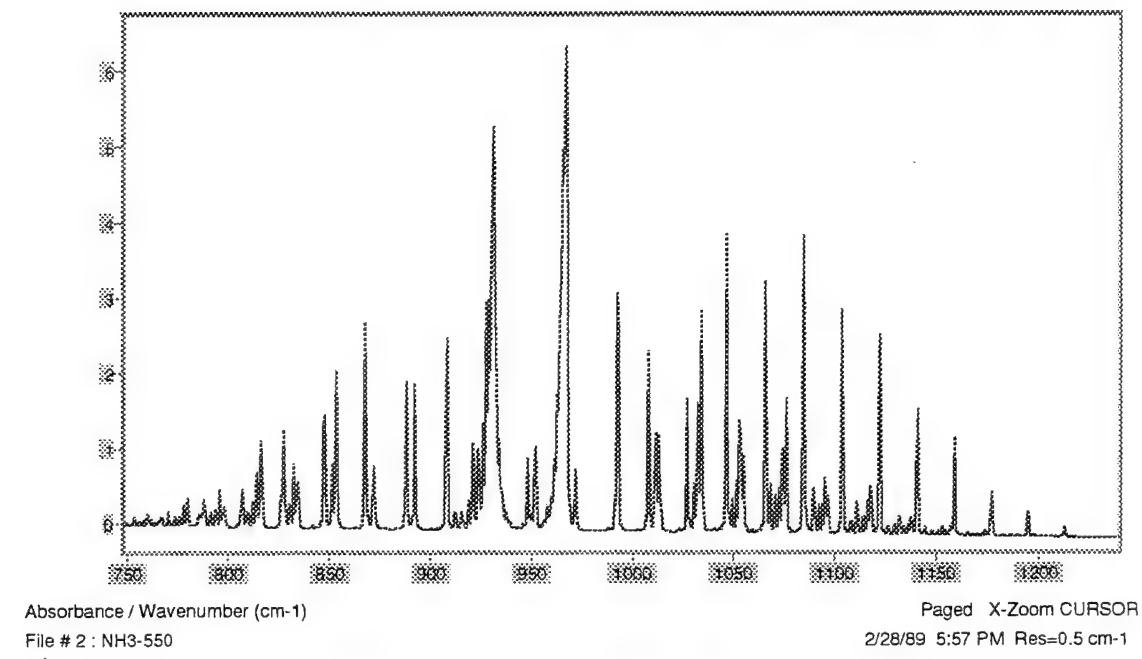


**Figure 17 Ammonia Reference Spectrum**

Scans near Monsanto, ratioed with s8061624. NH<sub>3</sub> is a different scale.

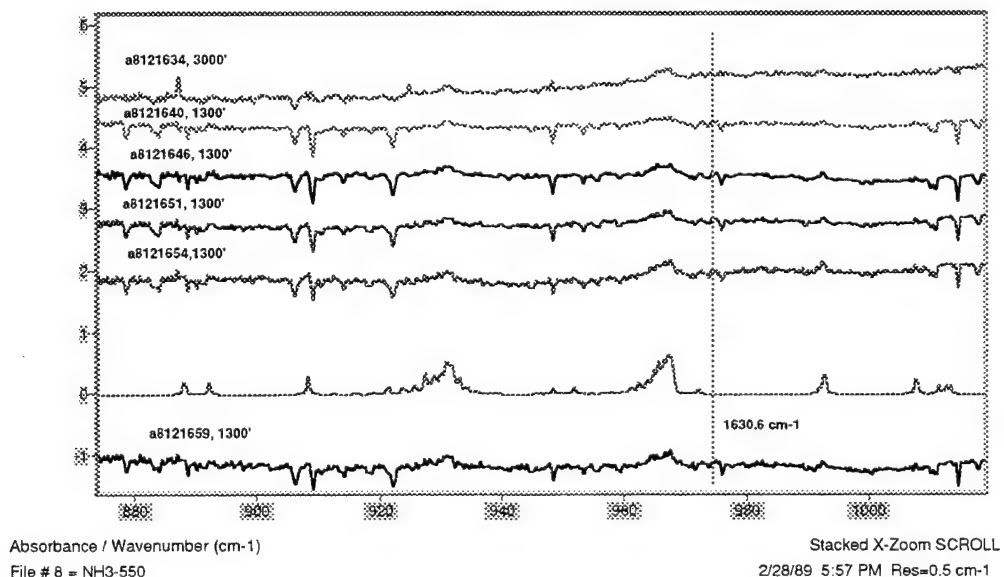


**Figure 18 Scans With Ammonia In Spectrum.**

## Quantitative Analysis of Ammonia at 1300 ft (1.07 ppm\*m, 10.9 ppb)

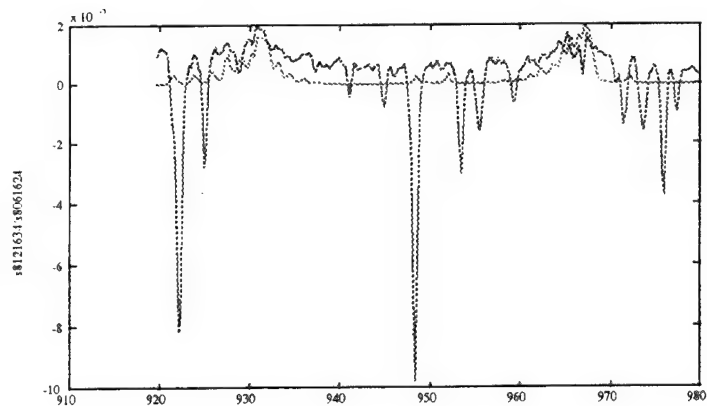


**Figure 19 CLS Analysis Of An Ammonia Spectrum**

### **5.3.3 Carbon Monoxide**

Also strong near the Fall River Trash Burner (Figure 20), the concentration estimates are 70 ppb. In the passive measurements this would be about 50 ppm\*m, but the strong lines are from 2000 to 2200  $\text{cm}^{-1}$  (Figure 21), where there is not much available energy. CO can be found in the following files: u8121807, u8121813, u8121817, u8121823, among others.

Scans near power plant overlaid w/ CO reference

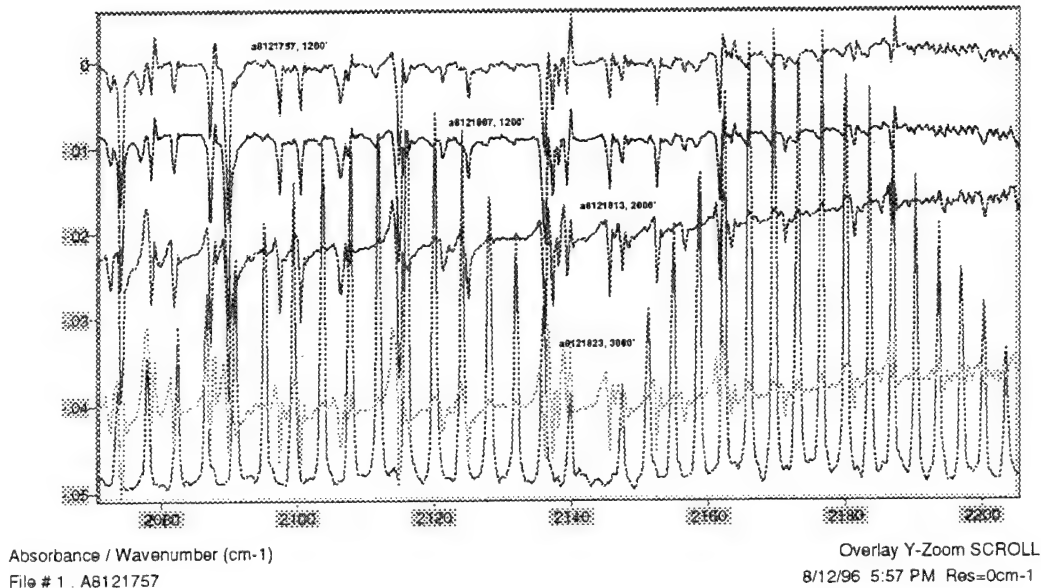


**Figure 20 CO Scans Near Power Plant.**

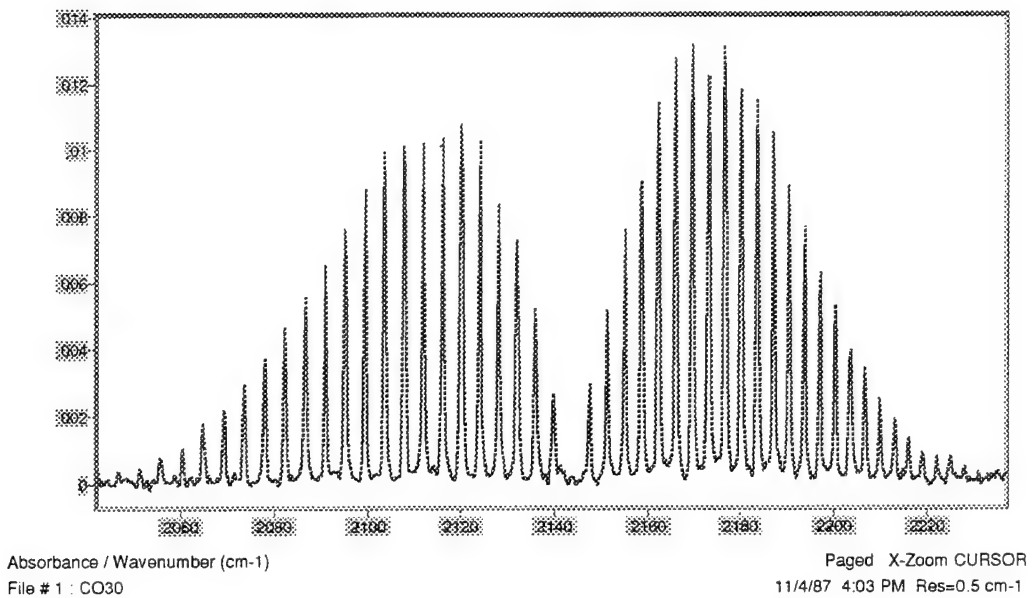


**Figure 21 CO Reference Spectrum**

#### 5.3.4 N<sub>2</sub>O

N<sub>2</sub>O is apparent in many spectra (Figure 22) such as u8121807 and preceding files, with a concentration of about 30 ppb. It is difficult to get an accurate measure in this region because of the intervening water lines, and the large CO<sub>2</sub> absorption nearby.

N<sub>2</sub>O (30 ppb) and (a8121807-a8121823) ; (a8121757-a8121823); relative absorbances.

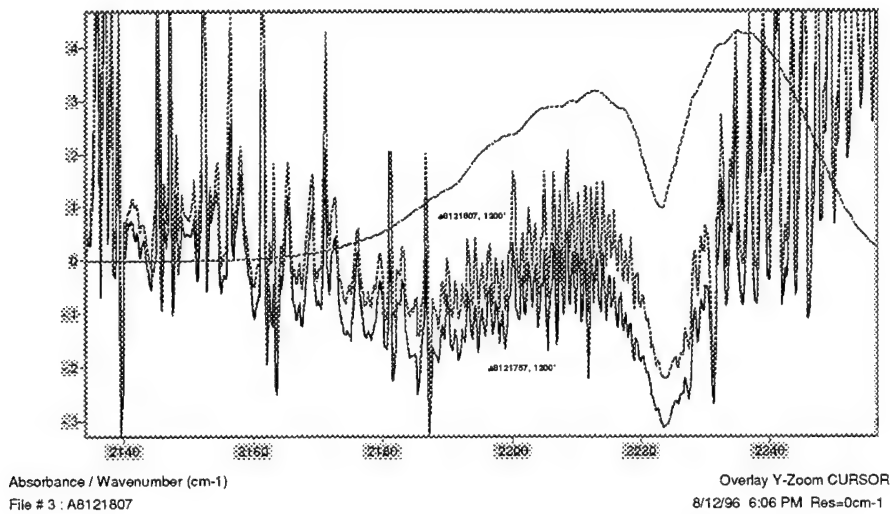


**Figure 22 N<sub>2</sub>O Downwind of Same Power Plant.**

#### 5.3.5 NO<sub>2</sub>

NO<sub>2</sub> is slightly visible near power plants, for example file U8061443 relative to U8061624 (Figure 23, and Figure 24), at about 35 ppb±50%. It is also apparent in scans near a power

plant, as can be seen in Figure 15. This measurement is moderately subjective, because of intervening strong water lines. As can be seen in the spectrum (Figure 25), the  $\text{NO}_2$  lines near  $1600 \text{ cm}^{-1}$  are not visible due to strong atmospheric absorption, so the  $2900 \text{ cm}^{-1}$  lines must be used.

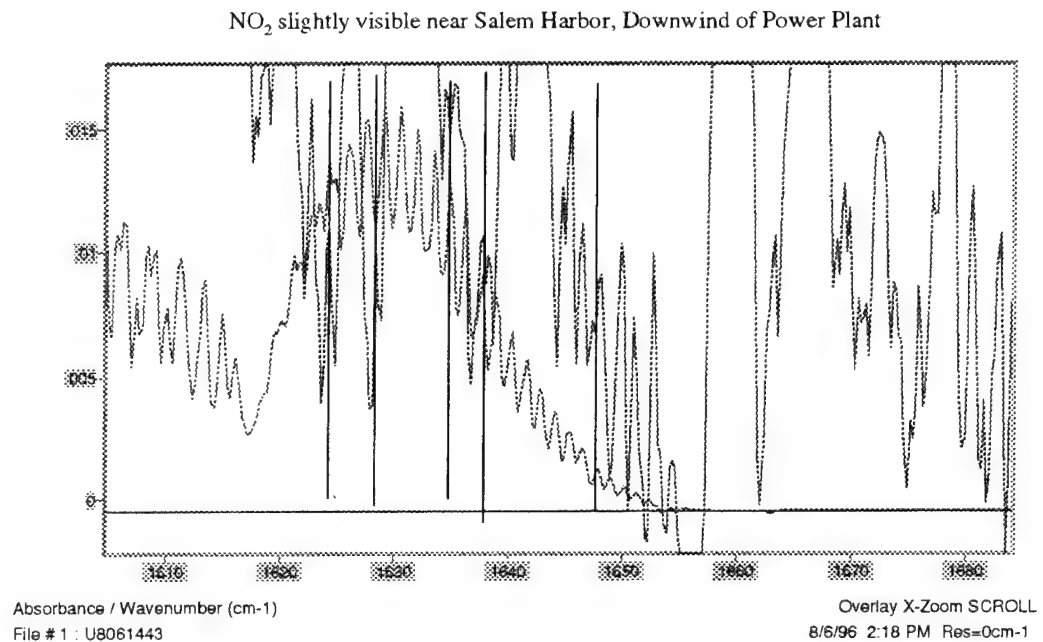


**Figure 23 Nitrogen Oxide Downwind Of Another Power Plant.**

a121757 and a121813 with 17 ppm\*m of NO<sub>2</sub>. Quabbin was reference.

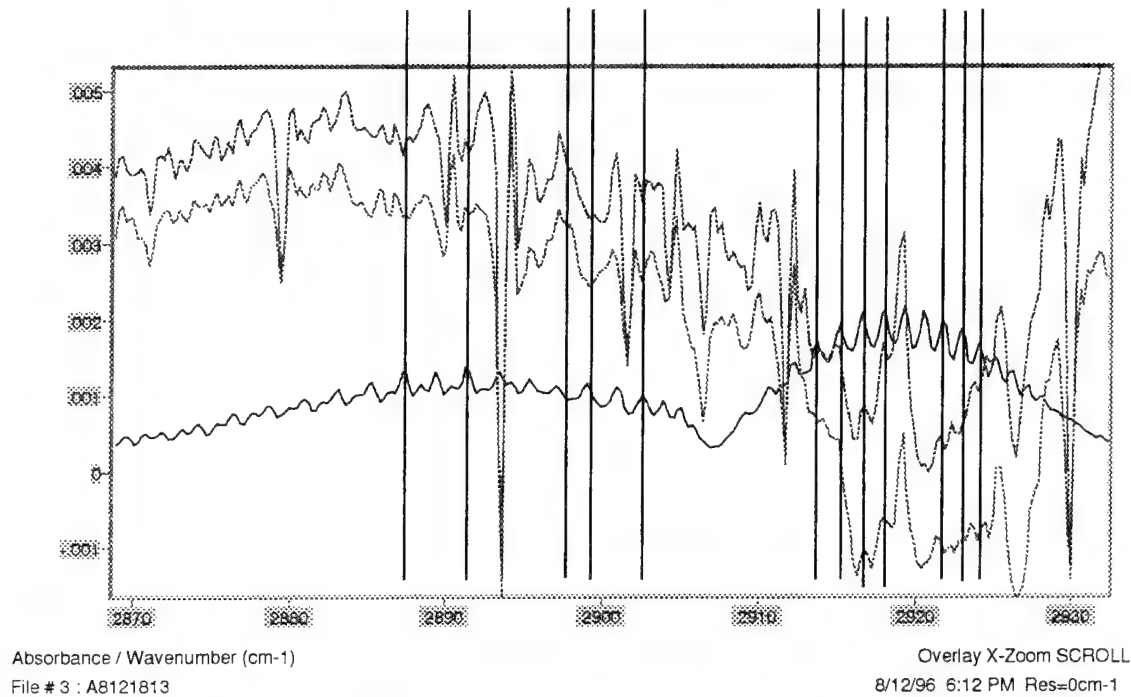


**Figure 24 Nitrogen Oxide Downwind Of Plant, w/ Reference.**

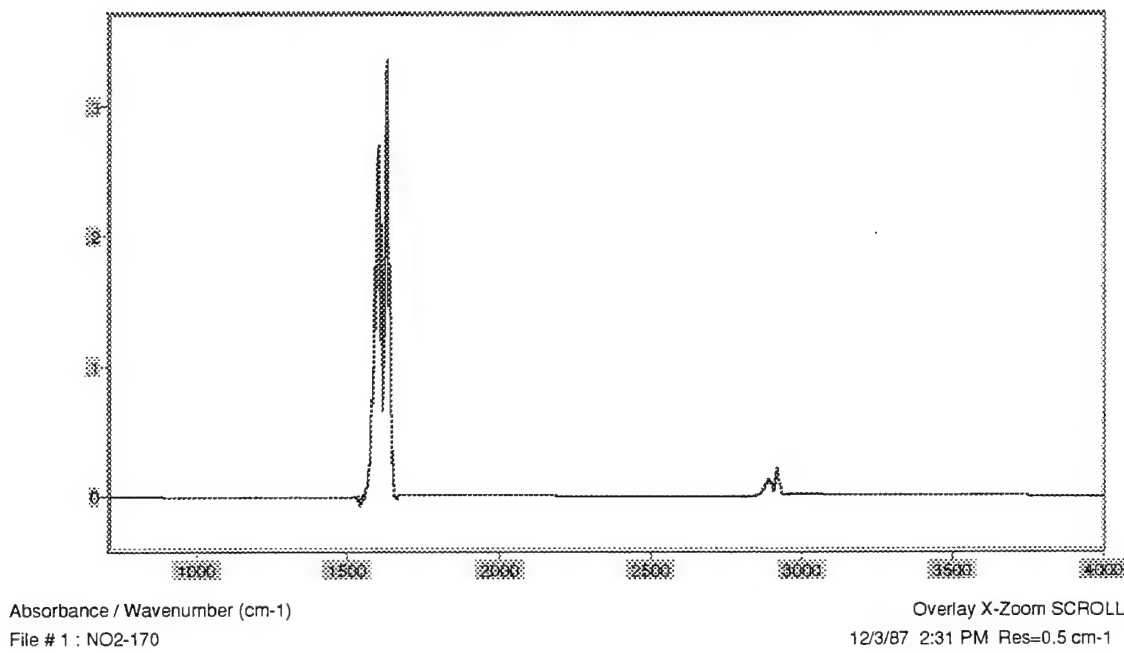


**Figure 25 NO<sub>2</sub> Reference.**

### 5.3.6 SO<sub>2</sub>

SO<sub>2</sub> has two sets of absorption lines, the 1100 cm<sup>-1</sup> lines and the 1350 cm<sup>-1</sup> lines (Figure 26). The higher frequency lines will be difficult to see amongst the water lines. The lower frequency lines will have amplitudes of 1 milliAu or less at the concentrations estimated here. This is at or below the noise level of a passive system. Figure 27 shows SO<sub>2</sub> in several measurements, although the levels are difficult to quantify because of the strong water lines nearby.

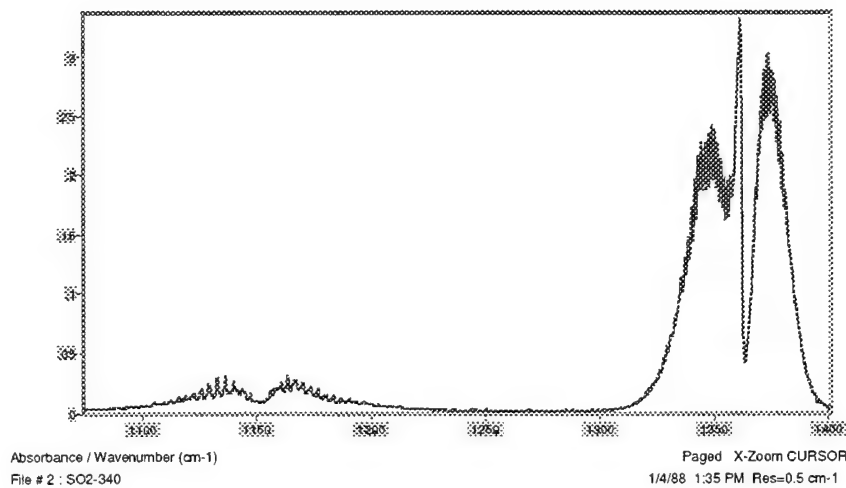


**Figure 26 SO<sub>2</sub> Reference**

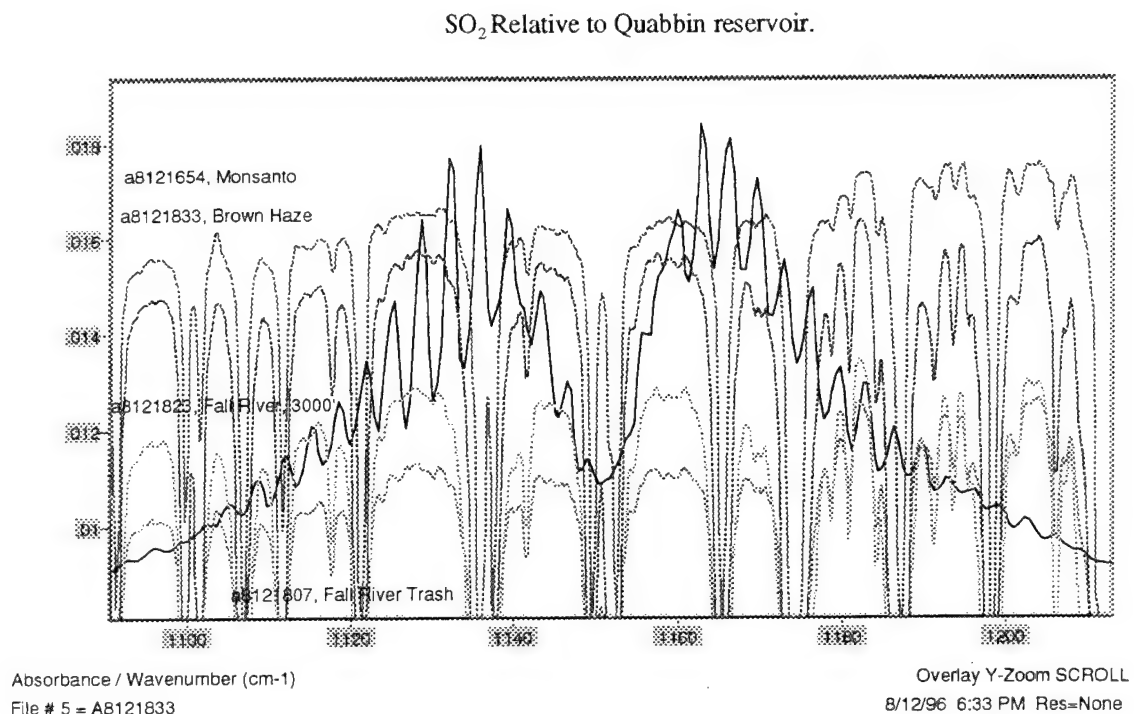


**Figure 27 SO<sub>2</sub> In Various Scans, w/ Reference**

#### 5.4 Implications for Passive Detection

In relating the extractive measurements to the corresponding passive data, several things must be considered. The extractive data, especially the data from varying altitudes at the same location, can be used to calculate the amount of chemical expected in the passive FTIR path (ppm\*meters). The amount of signal generated by this amount of chemical in a passive FTIR spectrum is affected by several things. The blackbody from the thermal radiation from the earth has most of its energy near 1000 cm<sup>-1</sup>. The amount of energy at wavelengths above 1500 cm<sup>-1</sup> is minimal. In addition, the atmosphere is not very transparent outside of the 8-12  $\mu$ m region, so that chemicals with spectra below 750 cm<sup>-1</sup> or above 1250 cm<sup>-1</sup> are not visible. For comparison to the passive measurements the spectral region of the greatest interest is the 800-1200 cm<sup>-1</sup> (Figure 28) where there are fewer interfering absorption lines and the atmosphere is more transparent. Unfortunately, this means that several of the chemicals apparent in the extractive measurements will not be visible using passive FTIR.

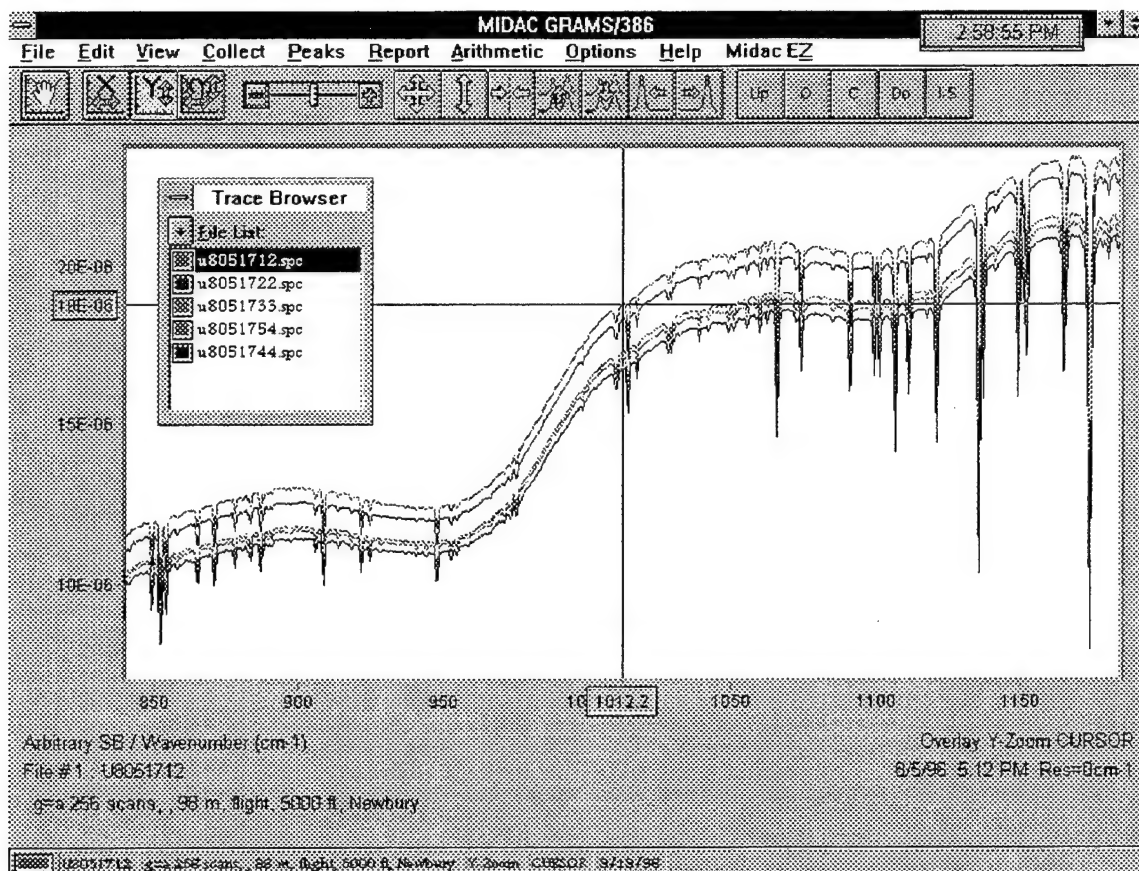


**Figure 28 Measured Spectra In Region Of Best Atmospheric Transmission**

#### **5.4.1 Ozone.**

From the measured data the amount of ozone when at 1000 meters AGL, shows the amount of ozone in the path would be 50 ppm\*m if conditions were similar. O<sub>3</sub> concentration nonattainment of the clean air act is > 0.12 ppm more than once per year. If concentrations were at that level, then 120 ppm\*m (a more visible amount) would be present. The absorbance of 50 ppm\*m of ozone is about 20 mAUs, and of course the 120 ppm\*m of ozone would have an absorbance of about 50 mAUs. Although ozone in high concentration would be detectable using passive FTIR, the problem of ozone spectra from the sky reflected off of the ground may complicate the quantitative determination of the concentration.

#### **5.4.2 Ammonia**

The estimated path length concentration product for ammonia, 10 ppm\*m, should have an absorbance of about 10 mAUs. This is a low level for passive measurements. Thus, for evidence of ammonia at this concentration it might be necessary to average a number of scans.

#### 5.4.3 SO<sub>2</sub>

SO<sub>2</sub> at the observed levels would probably not be visible with a passive system. For higher concentrations, such as the SO<sub>2</sub> concentrations required by the clean air act: (.14 ppm (24 hour avg.) ; 0.5 ppm (3 hr.) these levels can be exceeded only once per year) it may be visible. For example at 140 ppm\*m the peak absorbance of SO<sub>2</sub> is about 10 mAUs in the lines near 1160 cm<sup>-1</sup>.

#### 5.4.4 NO<sub>x</sub>

The concentration of N<sub>2</sub>O would be enough to see passively, except that there is little energy from thermal radiation near its absorption lines at 2200 cm<sup>-1</sup> (Figure 29), and the atmosphere is not transparent enough at these wavelengths for passive detection at long ranges. At the measured concentrations the lines near 1300 cm<sup>-1</sup> have an absorbance of about 10 mAUs, although they may not be visible through the atmosphere, and the lines near 1160 cm<sup>-1</sup> only have an absorbance of 0.2 mAUs at that concentration, far too low for passive detection.

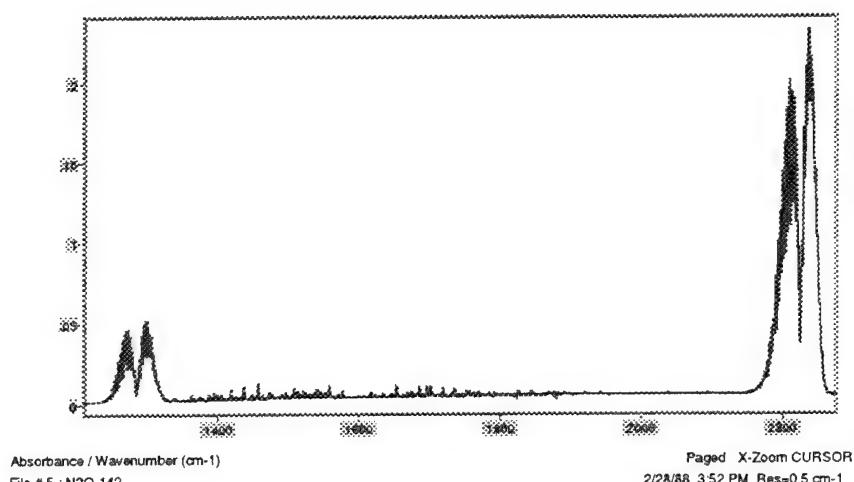


Figure 29 N<sub>2</sub>O Reference

## 6. Summer Airborne Passive Measurements

The summer passive measurements were much more eventful than the fall. Ozone was detected with reasonable regularity, and other chemicals such as methanol were also noted. The strength of the ozone signal was enough to attempt to quantify the result.

### 6.1 NESR During Flight

The in-flight NESR was estimated to be about  $1.3 \times 10^{-8}$ , in general, although some files were significantly worse. More problematic was ripples in the spectrum, probably due to shock or vibration. These ripples often are similar in structure to spectral lines, complicating detection.

## 6.2 Apparent Radiance Contrasts

The amount of radiance contrast is important because it is directly related to the amount of chemical that can be detected. If there is a large radiance contrast then a smaller amount of chemical can be detected.

The apparent radiance contrasts during the measurements of course varied widely, between zero and about  $1.2 \times 10^{-6} \text{ W/cm}^2 \text{sr cm}^{-1}$ , not counting the scans of sky.

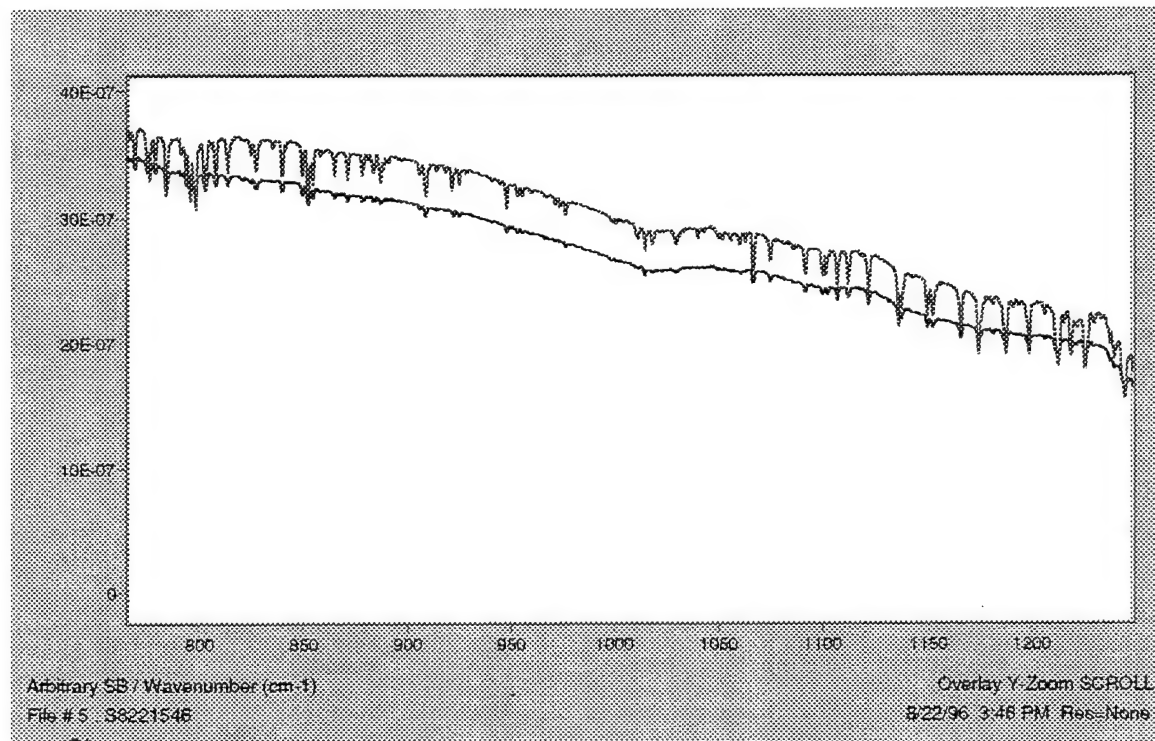


Figure 30 Apparent Radiance Contrasts During Flight Tests

## 6.3 Chemicals

During the flight tests in August at least three chemicals were detected. Ozone was detected in many spectra. There was also a probable detection of methanol, and possible ethanol. In addition, there was an unknown chemical in several spectra. This chemical had a noticeable absorption near  $1020 \text{ cm}^{-1}$ . Identification of this chemical was difficult, and it is possible that this was an instrumental artifact.

## s201818, less water

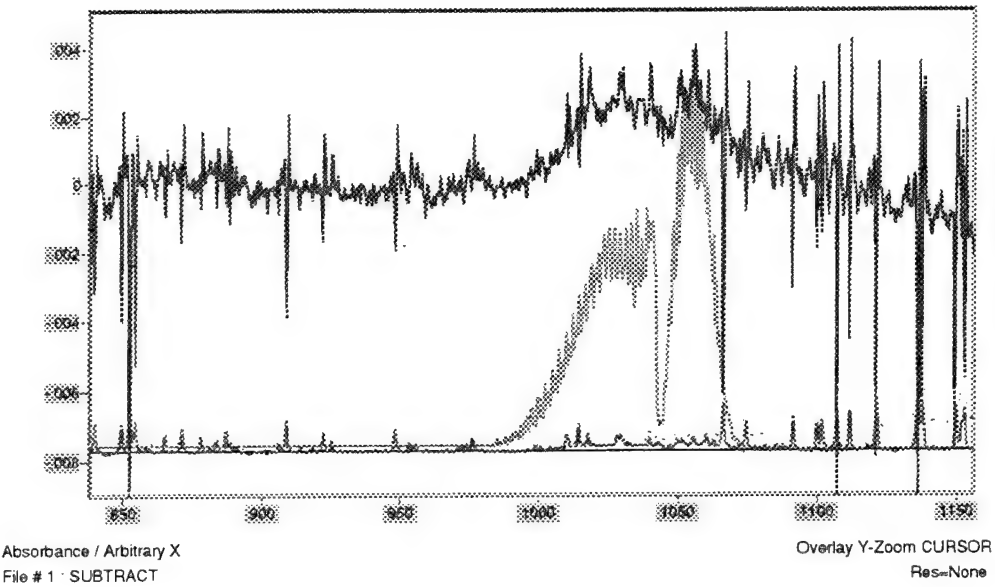
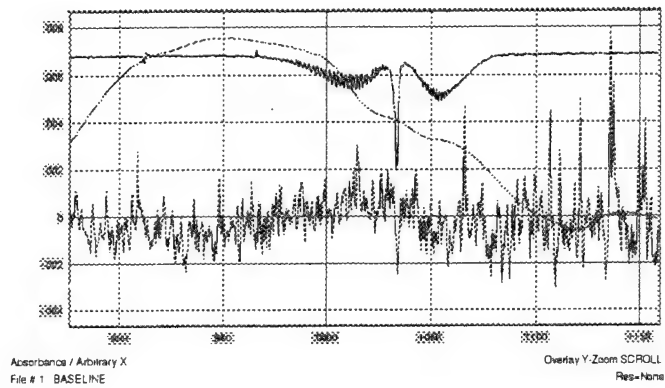


Figure 31 shows a clear detection of ozone after removal of the baseline, and manual removal of the water lines. The signal to noise ratio is very good in this average of 64 scans, especially after the water removal. When looking at uncoadded scans the ozone was not apparent even after removal of the water. However, when those scans were deresolved to  $4\text{ cm}^{-1}$  resolution the ozone was clearer, as can be seen in Figure 32.

Also methanol was noted in a few files, as can be seen in



s201843 #58. Possible Methanol in emission, perhaps Ethanol also.

Figure 33, and Figure 34. There might be a small amount of ethanol in those files also, but it is not clear.

In addition there was an unknown chemical detected during the August 20th return to Beverly Airport. It was difficult to correlate this to a specific chemical, and there is a chance that it was entirely instrumental in nature. The spectrum of the chemical can be seen in Figure 35.

s201818, less water

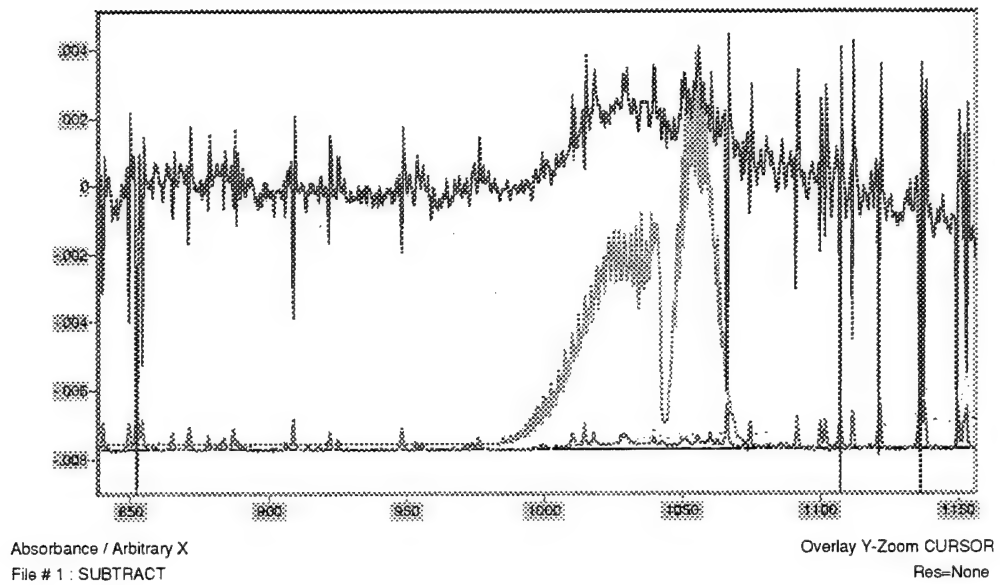


**Figure 31 Ozone Is Clearly Apparent After Water Removal, In Average Of 64 Scans**

s8201812 1 scan, subtract water, then deresolve  
to  $4 \text{ cm}^{-1}$

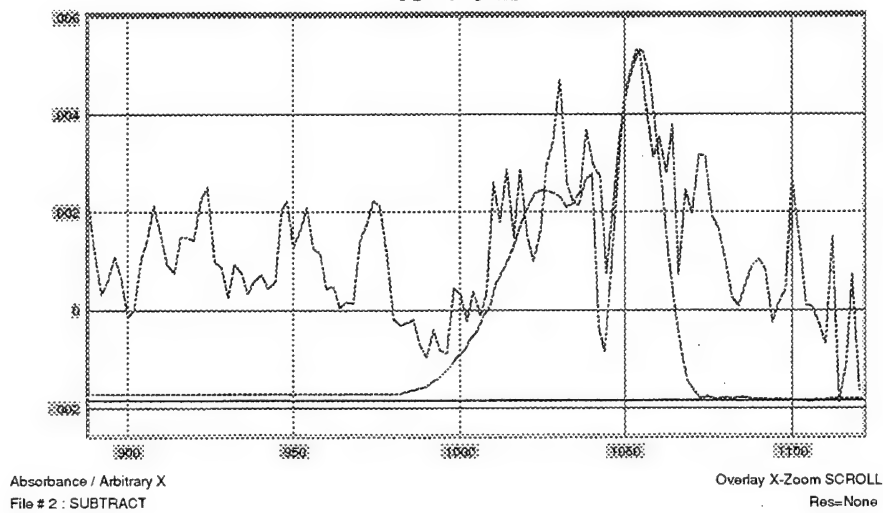


**Figure 32 Ozone Is More Detectable At Lower Resolution, Even In A Single Scan.**

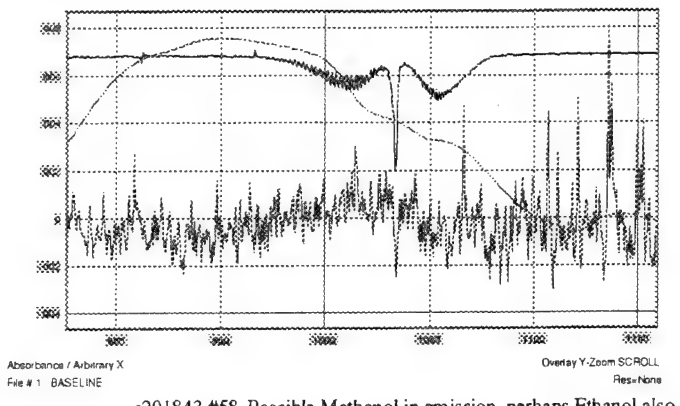


**Figure 33 Possible Methanol and Ethanol Detections**

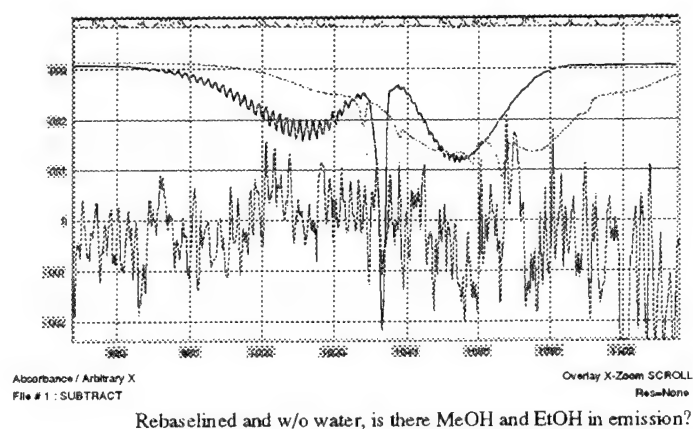


**Figure 34 Another Methanol Detection**

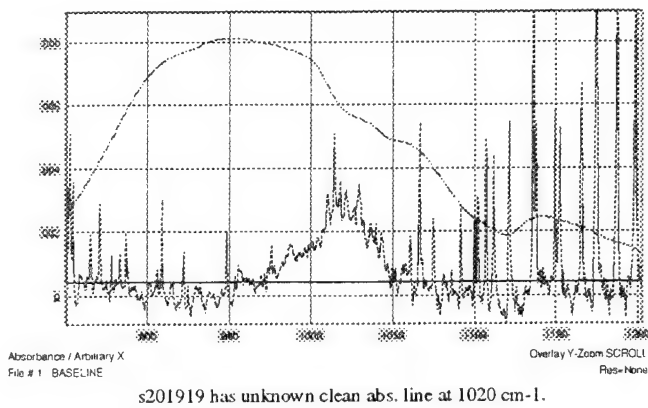


**Figure 35 Unknown Absorption Line.**

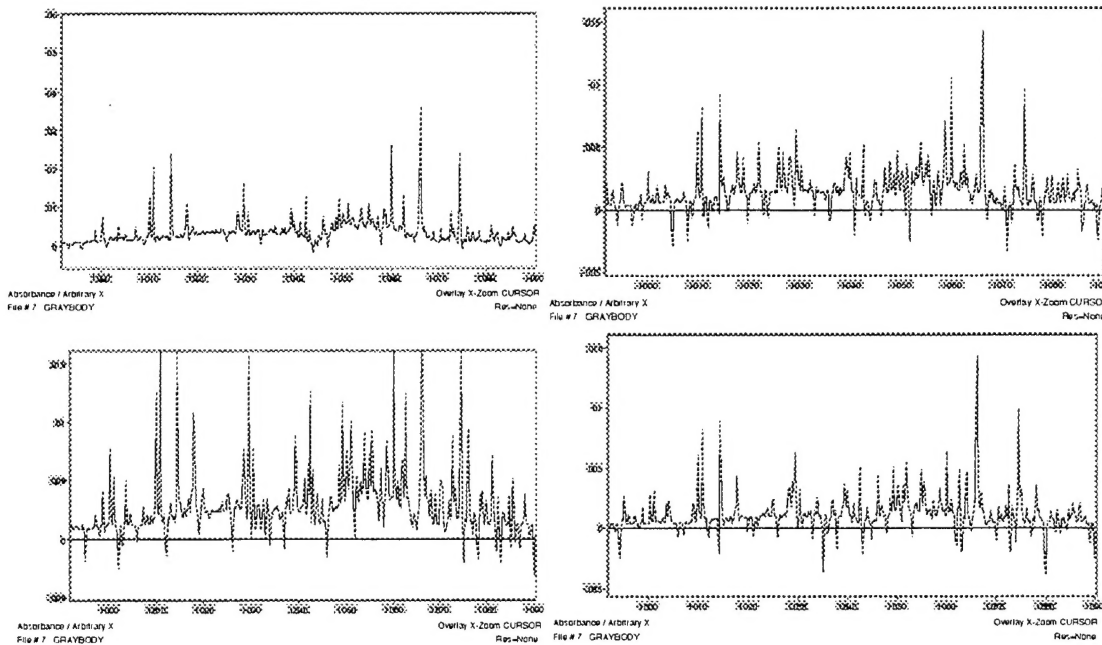
## 7. Conclusions for Passive FTIR for Environmental Monitoring

The detection limits of passive FTIR for detection of environmental chemicals are dependent on the absorption characteristics of the chemical, both in line strength and location. The amount of chemical detectable is also dependent on the temperature contrast, and so will vary depending on conditions.

### 7.1 Ozone

The calculated detection limits for ozone are 60 ppm\*m with a 5° contrast, and about 120 ppm\*m with a 2° contrast for an NESR of  $5 \times 10^{-9}$ . Both of these are a  $\Delta SR$  of  $5 \times 10^{-8}$  W/cm<sup>2</sup>sr cm<sup>-1</sup>, or a signal of 0.5% of the earth's radiance near room temperature. This compares well with the amount of ozone detected in the files. In a series of files from August 20, the apparent temperature difference was about 3½ degrees, the amount of ozone absorption in those files is about 12% of the magnitude of the 1066 water line, implying 160 ppm\*m of ozone if the water line was saturated, and 120 ppm\*m if the line was at an average level. The spectral radiance ( $\Delta SR$ ) in the measured data is  $7 \times 10^{-8}$  W/cm<sup>2</sup>sr cm<sup>-1</sup>. The estimated NESR in that file (composed of 64 coadded spectra) was  $6 \times 10^{-9}$  W/cm<sup>2</sup>sr cm<sup>-1</sup>.

120 ppm\*m of ozone; temperatures of 300° and 295°. 120 ppm\*m of ozone; temperatures of 300° and 298°.



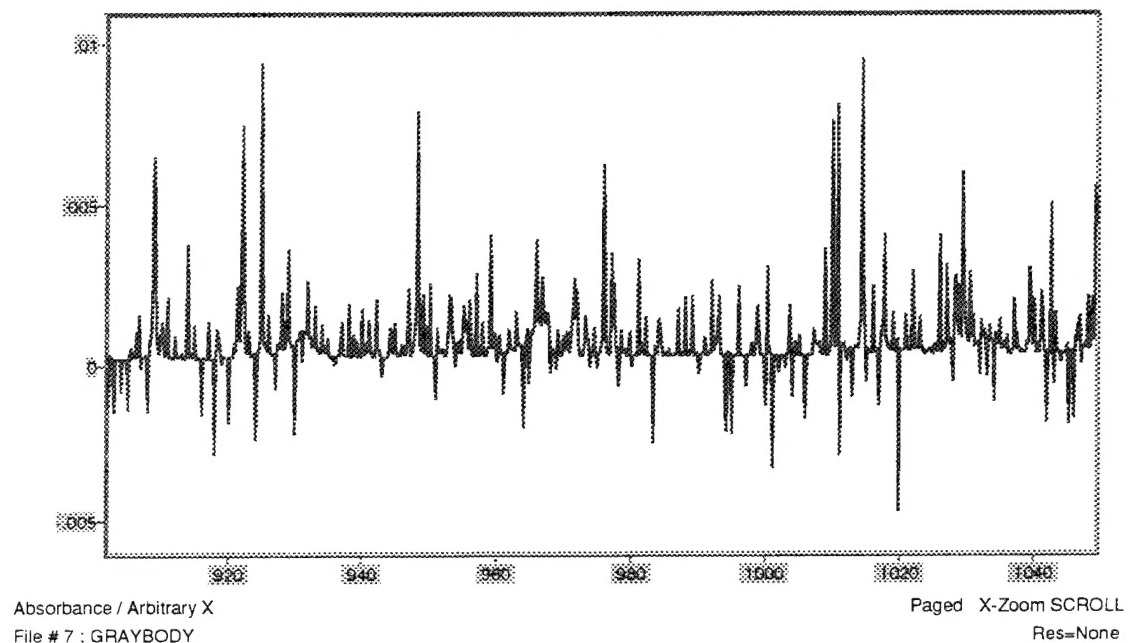
60 ppm\*m of ozone; temperatures of 300° and 295°. 60 ppm\*m of ozone; temperatures of 300° and 298°.

**Figure 36 Synthetically Generated Ozone Spectra w/ 1 Km Of Atmosphere.**

### 7.2 Ammonia

The calculated detection limits for ammonia are 30 ppm\*m for a 2° temperature difference. This is a  $\Delta SR$  of  $3 \times 10^{-8}$  W/cm<sup>2</sup>sr cm<sup>-1</sup>. Given the amount of ammonia in the extractive measurements (10 ppb) this should not have been detected in the passive

measurements. Figure 37 shows the synthetically generated spectrum of  $\text{NH}_3$  with 1 Km of atmosphere.

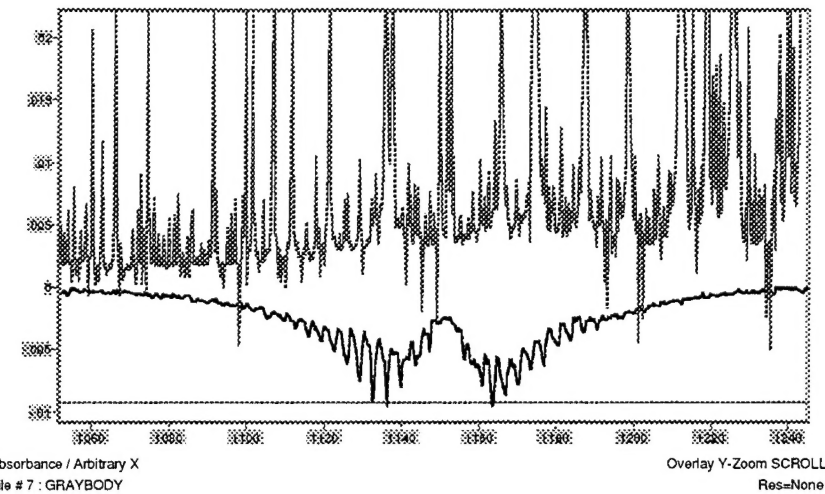


30 ppm\*m of ammonia, 300° and 298° ref. temps.

**Figure 37 Synthetically Generated Spectrum Of 30 ppm\*m Of  $\text{NH}_3$**

### 7.3 $\text{SO}_2$

The calculated detection limits for  $\text{SO}_2$  are about 500 ppm\*m for a 2° temperature difference and an NESR of  $5 \times 10^{-9} \text{ W cm}^2 \text{srcm}^{-1}$ . This high number is mostly due to the fact that weak lines are being used for the detection. Figure 38 shows the synthetically generated spectrum of  $\text{SO}_2$  with 1 Km of atmosphere and an instrument NESR of  $5 \times 10^{-9} \text{ W/cm}^2 \text{srcm}^{-1}$ .



500 ppm\*m of SO<sub>2</sub>, temperatures of 300° and 295° K.  
The lower trace is an SO<sub>2</sub> reference.

**Figure 38 Synthetically Generated SO<sub>2</sub> Spectrum And 1 Km Of Atmosphere**

#### 7.4 N<sub>2</sub>O

The detection limits for N<sub>2</sub>O are 100 ppm\*m for a temperature difference of 2°, and the 5x10<sup>-9</sup> W/cm<sup>2</sup>srcm<sup>-1</sup> NESR.

#### 7.5 Methanol

The detection limits for methanol are about 40 ppm\*m for the usual 2° temperature contrast and 5x10<sup>-9</sup> W/cm<sup>2</sup>srcm<sup>-1</sup> NESR. The source of methanol does not have to be a chemical facility, it can also be a result of burning material. This is consistent with the fact that the spectra of the presumed detections are in emission (hotter than the background), while all the other lines in those spectra are in absorption.

#### 7.6 Aliphatic Hydrocarbons

A number of aliphatic hydrocarbons have spectra in the 800-1200 cm<sup>-1</sup> region accessible to passive FTIR. Ethylene, isobutane, gasoline, etc. are in principle detectable. Ethylene should be reasonably detectable, but has a water line close enough to degrade detection limits. Without the water line the detection limit should be about 30 ppm\*m for Ethylene. Isobutane only has relatively weak lines in the far-IR, so that the detection limits are relatively high (~100 ppm\*m). Gasoline is a mixture of hydrocarbons, some of which have spectral features in the region of interest, but the calculation of the exact detectability requires specific knowledge of the mixture composition.

#### 7.7 Aromatic Hydrocarbons

Aromatic Hydrocarbons, such as Benzene and Toluene are of interest to the EPA. Toluene has a very strong absorption line at 729 cm<sup>-1</sup>, but unfortunately this line is strongly obscured by water. A clever algorithm might be able to use this line effectively, but it would

have to remove the effects of water first. The other line that could be used would limit detection to an impractically high level.

Benzene has a good line at 1036, which could be used. The detection limit for Benzene should be roughly 40 ppm\*m, or 40 ppb over a 1000 meter path.

### **7.8 Other**

The above results can be generalized to provide a rough estimate for detection limits for any chemical. Detectable change in spectral radiance, for a chemical, without interferents, can be generalized. Given an assumed temperature contrast this can be generalized further to a minimum detectable absorbance. For a 2° temperature contrast and an instrument with an NESR of  $5 \times 10^{-9}$  W/cm<sup>2</sup>sr cm<sup>-1</sup> the minimum detectable absorbance is roughly 0.003, without accounting for interferents, or atmospheric transmission. This result can then be applied to each chemical, for an initial estimate of detectability. To calculate detection limits more accurately the specific spectra, the expected atmosphere, and the specific instrument must be accounted for.

### **7.9 Conclusion**

Passive FTIR can be used to monitor several chemicals in the environment at levels appropriate for environmental monitoring, especially ozone. Although ozone can be problematic because of the contribution of sky reflection, ozone was detected at levels estimated to be 120 ppb. The detection limit is about one half of this, and could be reduced further with improved methods of water line removal. An FTIR with a lower effective NESR (e.g. better vibration isolation) would also improve those detection limits. Moderately high levels (<50 ppb) of other chemicals can also be seen, depending on the environmental conditions. Although a trained spectroscopist is always the best judge of the presence of a chemical, algorithms can be developed to do a reasonable job of automated detection. In passive detection the algorithm can be separated into two parts: the  $I_0$  removal, and the pattern recognition.

The  $I_0$  removal should be as close as possibly related to the IRF of the specific instrument, and the radiance, both internal and external, into the detector. The more radiometrically accurate the background removal, the more accurate it will be. This program developed a method of background removal 30% better than the previous technique.

The pattern recognition used for environmental monitoring could be either CLS, or a more sophisticated method such as PCA. CLS is the more straightforward to use, and more accepted in the regulatory community, PCA, with a sufficient training, has the potential for greater sensitivity.